Krishnaswami, G. S., Phatak, S. S., Sachdev, S., & Thyagaraja, A. (2020). Nonlinear dispersive regularization of inviscid gas dynamics. *AIP Advances*, *10*(2), [025303]. https://doi.org/10.1063/1.5133720

Nonlinear dispersive regularization of inviscid gas dynamics

Cite as: AIP Advances **10**, 025303 (2020); https://doi.org/10.1063/1.5133720
Submitted: 25 October 2019 . Accepted: 15 January 2020 . Published Online: 03 February 2020

Govind S. Krishnaswami, Sachin S. Phatak, Sonakshi Sachdev, and A. Thyagaraja

Nonlinear dispersive regularization of inviscid gas dynamics

Cite as: AIP Advances 10, 025303 (2020); doi: 10.1063/1.5133720
Submitted: 25 October 2019 • Accepted: 15 January 2020 •
Published Online: 3 February 2020

Govind S. Krishnaswami,[1,a] Sachin S. Phatak,[1,b] Sonakshi Sachdev,[1,b] and A. Thyagaraja[2,c]

AFFILIATIONS

[1]Chennai Mathematical Institute, SIPCOT IT Park, Siruseri 603103, India
[2]Astrophysics Group, University of Bristol, Bristol BS8 1TL, United Kingdom

[a]Author to whom correspondence should be addressed: govind@cmi.ac.in
[b]Electronic addresses: phatak@cmi.ac.in and sonakshi@cmi.ac.in
[c]Electronic mail: athyagaraja@gmail.com

ABSTRACT

Ideal gas dynamics can develop shock-like singularities with discontinuous density. Viscosity typically regularizes such singularities and leads to a shock structure. On the other hand, in one dimension, singularities in the Hopf equation can be non-dissipatively smoothed via Korteweg–de Vries (KdV) dispersion. In this paper, we develop a minimal conservative regularization of 3D ideal adiabatic flow of a gas with polytropic exponent γ. It is achieved by augmenting the Hamiltonian by a capillarity energy $\beta(\rho)(\nabla\rho)^2$. The simplest capillarity coefficient leading to local conservation laws for mass, momentum, energy, and entropy using the standard Poisson brackets is $\beta(\rho) = \beta_*/\rho$ for constant β_*. This leads to a Korteweg-like stress and nonlinear terms in the momentum equation with third derivatives of ρ, which are related to the Bohm potential and Gross quantum pressure. Just like KdV, our equations admit sound waves with a leading cubic dispersion relation, solitary waves, and periodic traveling waves. As with KdV, there are no steady continuous shock-like solutions satisfying the Rankine–Hugoniot conditions. Nevertheless, in one-dimension, for $\gamma = 2$, numerical solutions show that the gradient catastrophe is averted through the formation of pairs of solitary waves, which can display approximate phase-shift scattering. Numerics also indicate recurrent behavior in periodic domains. These observations are related to an equivalence between our regularized equations (in the special case of constant specific entropy potential flow in any dimension) and the defocusing nonlinear Schrödinger equation (cubically nonlinear for $\gamma = 2$), with β_* playing the role of $\hbar^2$. Thus, our regularization of gas dynamics may be viewed as a generalization of both the single field KdV and nonlinear Schrödinger equations to include the adiabatic dynamics of density, velocity, pressure, and entropy in any dimension.

I. INTRODUCTION

Gas dynamics has been an active area of research with applications to high-speed flows, aerodynamics, and astrophysics. The equations of ideal compressible flow are known to encounter shock-like singularities with discontinuities in density, pressure, or velocity.[1] These singularities are often resolved by the inclusion of viscosity. However, as the Korteweg–de Vries (KdV) equation ($u_t + uu_x = \varepsilon u_{xxx}$) illustrates, such singularities in the one-dimensional (1D) Hopf (or kinematic wave) equation $u_t + uu_x = 0$ can also be regularized conservatively via dispersion,[2] as in dispersive shock wave theory (see Refs. 1 and 3–5 and references therein) with applications to undular bores in shallow water and blast waves in Bose–Einstein condensates. In this paper, we develop a minimal conservative regularization of ideal gas dynamics, which we refer to as R-gas dynamics. Somewhat analogous conservative "rheological" regularizations of vortical singularities in ideal Eulerian hydrodynamics, magnetohydrodynamics, and two-fluid plasmas have been developed in Refs. 6–8. The current work may be regarded as a way of extending the single-field KdV equation to include the dynamics of density, velocity, and pressure and also to dimensions higher than one. There is, of course, a well-known generalization of KdV to two dimensions, the Kadomtsev–Petviashvili (KP) equation.[9] However, unlike KP, our regularized equations are rotation-invariant and valid in any dimension. Now, recall[10] that the dispersive regularization term in the KdV equation $u_t - 6uu_x + u_{3x} = 0$ arises from the gradient

energy term in the Hamiltonian $H = \int (u^3 + (1/2)u_x^2)\, dx$ upon use of the Poisson brackets (PB) $\{u(x), u(y)\} = \partial_x \delta(x - y)$. In fact, KdV does not conserve mechanical and capillarity energies separately.[11,12] By analogy with this, we obtain our regularized model by augmenting the Hamiltonian of ideal adiabatic flow of a gas with polytropic exponent γ by a density gradient energy $\beta(\rho)(\nabla\rho)^2$. Such a term arose in the work of van der Waals and Korteweg[13–16] in the context of capillarity, but can be important even away from interfaces in any region of rapid density variation, especially when dissipative effects are small, such as in weak shocks, cold atomic gases, superfluids, and collisionless plasmas. It has also been used to model liquid–vapor phase transitions and in the thermomechanics of interstitial working.[15] We argue that the simplest choice of capillarity coefficient that leads (using the standard Poisson brackets) to local conservation laws for mass, momentum, energy, and entropy (with the standard mass, momentum, and entropy densities) is $\beta(\rho) = \beta_*/\rho$, where β_* is a constant. By contrast, the apparently simpler option of taking $\beta(\rho)$ constant leads, in one dimension, to a KdV-like linear dispersive term ρ_{xxx} in the velocity equation, but results in a momentum equation that, unlike KdV,[11] is *not* in conservation form for the standard momentum density ρu. A consequence of the constitutive law $\beta = \beta_*/\rho$ is that the ideal momentum flux $\rho u^2 + p$ is augmented by a stress $-\beta_*(\rho_{xx} - \rho_x^2/\rho)$ corresponding to a Korteweg-type *grade* 3 elastic material.[15,16] This leads to new nonlinear terms in the momentum equation with third derivatives of ρ, somewhat reminiscent of KdV. One of the effects of these nonlinear dispersive terms is to allow for "upstream influence,"[17] which is forbidden by the hyperbolic equations of inviscid gas dynamics under supersonic conditions. Interestingly, our regularization term is also related to the quantum mechanical Bohm potential[18] and Gross quantum pressure (p. 476 of Ref. 19) encountered in superfluids. Moreover, unlike KdV, our equations extend in a natural way to any dimension. Remarkably, for potential flow ($\mathbf{v} = \nabla\phi$) in the isentropic case (globally constant entropy and $p \propto \rho^\gamma$), the R-gas dynamic equations may be transformed into the nonlinear Schrödinger equation (NLSE) via the Madelung transformation[20] $\psi = \sqrt{\rho}\exp\left(i\phi/2\sqrt{\beta_*}\right)$ with β_* playing the role of $\hbar^2$. This equivalence, which may be regarded as a conservative analog of the Cole–Hopf transformation for Burgers, applies in any dimension and results in a defocusing NLSE with $|\psi|^{2(\gamma-1)}\psi$ nonlinearity so that one obtains the celebrated cubic NLSE for $\gamma = 2$. The latter is known to admit an infinite number of conservation laws and display recurrence. It is noteworthy that the *quantum* version of the 1D cubic NLSE (Lieb–Liniger model) has recently been given a hydrodynamical description (generalized hydrodynamics[21,22]) with infinitely many local conservation laws and has been used to model 1D gases of ultracold rubidium atoms that retain memory of their initial state.[23]

A brief summary of this paper and its organization follows. We begin in Sec. II by giving the Lagrangian (in terms of Clebsch variables) and Hamiltonian formulations and equations of motion (EOM) of adiabatic R-gas dynamics in three dimensions. The mass, momentum, energy, and entropy equations are all expressed in conservation form. In Sec. III, we specialize to one dimension and discuss the special case of constant entropy (isentropic/barotropic) flow in which case the velocity equation also acquires a conservation form. Sound waves are discussed in Sec. IV A and shown to be governed at long wavelengths by a cubic dispersion relation similar to that of the linearized KdV equation. In Sec. IV B, the local conservation laws are used to reduce the determination of steady and traveling wave solutions in one dimension to a single quadrature of a generalization of the Ermakov–Pinney equation. A mechanical analogy and phase plane analysis is used to show that the only such nonconstant bounded solutions are cavitons (in density) and periodic waves. While these results hold for any value of γ, for $\gamma = 2$, closed-form sech^2 and cnoidal wave solutions are obtained, physically interpreted and compared with the corresponding KdV solutions. We also propose a simple physical procedure to produce a caviton. Aside from overall scales, steady solutions are parameterized by a pair of dimensionless shape parameters: a Mach number and a curvature. A parabolic embedding and a virial theorem for steady flows are given in Appendix C. In Sec. V A, the weak form of the R-gas dynamic equations is given, and in Sec. V B, an attempt is made to find a steady normal shock-like profile in three dimensions by patching half a 1D caviton with a constant solution. However, it is shown that there are no such continuous profiles that satisfy all the Rankine–Hugoniot (RH) conditions, though it may be possible to satisfy the mass flux condition alone. To study more general time-dependent solutions of R-gas dynamics and the evolution of initial conditions (ICs) that could lead to shock-like discontinuities, we set up in Sec. VI, a semi-implicit spectral numerical scheme for the isentropic R-gas dynamic equations with periodic boundary conditions (BCs) in one dimension. For $\gamma = 2$, our numerical solutions indicate that our regularization evades the gradient catastrophe through the formation of a pair of solitary waves at the top and bottom of a velocity profile with a steep negative gradient. Although we do not observe a KdV-like solitary wave train, these solitary waves can suffer collisions and approximately reemerge with a phase shift. We also observe a rapid decay of energy with mode number and recurrent behavior with the Rayleigh quotient fluctuating between bounded limits, indicating an effectively finite number of active Fourier modes. In Sec. VII, we use a canonical transformation to reformulate 3D adiabatic R-gas dynamics in terms of a complex scalar field coupled to an entropy field and three Clebsch potentials. For isentropic potential flows, this formulation shows that R-gas dynamics for any γ reduces to a defocusing 3D NLSE. In Sec. VII A, the regularized Bernoulli equation is used to show that steady R-gas dynamic solutions map to solutions of NLSE with harmonic time dependence, with the $\gamma = 2$ caviton in one dimension corresponding to the dark soliton of the cubic NLSE. In Sec. VII B, we relate the conserved quantities and bounded Rayleigh quotient of NLSE to their R-gas dynamic analogs. This connection lends credence to our numerical observations, since the cubic NLSE with periodic BCs in one dimension is known to possess an infinity of conserved quantities in involution.[24] We conclude with a discussion in Sec. VIII.

II. HAMILTONIAN AND LAGRANGIAN FORMULATIONS OF 3D R-GAS DYNAMICS

It is well-known[1] that adiabatic dynamics of an ideal gas with constant specific heat ratio $\gamma = c_p/c_v$ is governed by the continuity, momentum, and internal energy equations

$$\rho_t + \nabla\cdot(\rho\mathbf{v}) = 0, \quad (\rho v_i)_t + \partial_j(p\delta_{ij} + \rho v_i v_j) = 0,$$

and

$$\left(\frac{p}{\gamma-1}\right)_t + p\nabla\cdot\mathbf{v} + \nabla\cdot\left(\frac{p\mathbf{v}}{\gamma-1}\right) = 0 \tag{1}$$

with the temperature in energy units given by $T = mp/\rho$ for a molecular mass m. In adiabatic flow, specific entropy (per unit mass) is advected ($D_t s \equiv \partial_t s + \mathbf{v}\cdot\nabla s = 0$), while the entropy per unit volume is locally conserved, $\partial_t(\rho s) + \nabla\cdot(\rho s\mathbf{v}) = 0$. Although the terms "reversibly adiabatic" and "isentropic" are often used interchangeably, in this paper, we use adiabatic for $D_t s = 0$ and isentropic for the special case where s is a global constant. For adiabatic flow, ρ and p may be taken as independent variables with s being a function of them. For a polytropic gas, $s = c_v \log((p/\bar{p})/(\rho/\bar{\rho})^\gamma)$, where $\bar{p}, \bar{\rho}$ are reference values. These equations follow from the Hamiltonian

$$H_{\text{ideal}} = \int\left[\frac{1}{2}\rho\mathbf{v}^2 + \frac{p}{\gamma-1}\right]d\mathbf{r} \tag{2}$$

and Hamilton's equations $\dot{f} = \{f, H\}$ using the (non-zero) non-canonical Poisson brackets (PB)[25]

$$\{\mathbf{v}(\mathbf{x}), \rho(\mathbf{y})\} = \nabla_y\delta(\mathbf{x}-\mathbf{y}), \quad \{\mathbf{v}(\mathbf{x}), s(\mathbf{y})\} = \frac{\nabla s}{\rho}\delta(\mathbf{x}-\mathbf{y}),$$

and

$$\{v_i(\mathbf{x}), v_j(\mathbf{y})\} = \frac{\varepsilon_{ijk}w_k}{\rho}\delta(\mathbf{x}-\mathbf{y}), \tag{3}$$

where $\mathbf{w} = \nabla\times\mathbf{v}$ is the vorticity. Our conservative regularization involves adding a density gradient term to the Hamiltonian while retaining the same PBs,

$$H = \int \mathscr{E}\, d\mathbf{r} \equiv \int\left[\frac{1}{2}\rho\mathbf{v}^2 + \frac{p}{\gamma-1} + \frac{\beta_*}{2}\frac{(\nabla\rho)^2}{\rho}\right]d\mathbf{r}. \tag{4}$$

The density gradient energy, which could arise from capillarity,[13,14] has been chosen $\propto(\nabla\rho)^2$ to ensure positivity and parity conservation and to prevent discontinuities in density, so as to conservatively regularize shock-like discontinuities. It involves the capillarity coefficient $\beta(\rho) = \beta_*/\rho$, where β_* is a constant with dimensions L^4T^{-2}. β_* can be taken as λ^2c^2, where λ is a short-distance cutoff and c is a typical speed. This is the simplest form for $\beta(\rho)$ that ensures the mass, momentum, and energy equations are all in conservation form for the ideal mass and momentum densities. It also leads to other excellent properties such as a transformation to the NLSE for isentropic potential flow.

The continuity and entropy equations following from (4) and (3) are as in the ideal model. The momentum and consequently the velocity equation, however, differ due to the presence of a capillary force term $\beta_*\mathbf{F}$,

$$\begin{aligned}\mathbf{v}_t + \mathbf{v}\cdot\nabla\mathbf{v} + \frac{\nabla p}{\rho} &= \beta_*\mathbf{F} = \beta_*\nabla\left[\frac{1}{2}\frac{(\nabla\rho)^2}{\rho^2} + \nabla\cdot\left(\frac{\nabla\rho}{\rho}\right)\right]\\ &= \beta_*\nabla\left[\frac{\nabla^2\rho}{\rho} - \frac{1}{2}\frac{(\nabla\rho)^2}{\rho^2}\right] = 2\beta_*\nabla\left(\frac{\nabla^2\sqrt{\rho}}{\sqrt{\rho}}\right).\end{aligned} \tag{5}$$

Remarkably, $\beta_*\mathbf{F} = \beta_*\nabla\Phi$ is a gradient so that for barotropic flow ($\nabla p/\rho = \nabla h$), it augments the specific enthalpy $h \to h + \beta_*\Phi$. Thus, the vorticity evolves exactly as in ideal gas dynamics (in other words, we only regularize the "potential" part of the velocity and do not deal with vortical singularities as in Refs. 6 and 7). Thus, Kelvin's theorem would apply in R-gas dynamics, unchanged. The momentum and velocity equations may be expressed in terms of a regularized stress tensor,

$$\partial_t(\rho v_i) + \partial_j(\rho v_i v_j + \sigma_{ij}) = 0$$

and

$$\partial_t v_i + v_j\partial_j v_i = -\frac{1}{\rho}\partial_j\sigma_{ij},$$

where

$$\sigma_{ij} = p\,\delta_{ij} + \beta_*\left(\frac{(\partial_i\rho)(\partial_j\rho)}{\rho} - \partial_i\partial_j\rho\right). \tag{6}$$

The scalar part of σ defines a regularized pressure p_* that includes the Gross "quantum pressure,"[19]

$$p_* = \frac{1}{d}\,\mathrm{tr}\,\sigma = p + \frac{\beta_*}{d}\left(\frac{(\nabla\rho)^2}{\rho} - \nabla^2\rho\right), \quad \text{where } d = 3. \tag{7}$$

The energy equation for the energy density $\mathscr{E}$ defined in (4) is given by

$$\begin{aligned}&\mathscr{E}_t + \nabla\cdot\left(\frac{\rho\mathbf{v}^2}{2}\mathbf{v} + \frac{\gamma}{\gamma-1}p\mathbf{v}\right)\\ &\quad + \beta_*\nabla\cdot\left[\frac{\nabla\rho}{\rho}\nabla\cdot(\rho\mathbf{v}) - \rho\mathbf{v}\nabla\cdot\left(\frac{\nabla\rho}{\rho}\right) - \frac{\rho\mathbf{v}}{2}\frac{(\nabla\rho)^2}{\rho^2}\right] = 0.\end{aligned} \tag{8}$$

The fact that (8) is in local conservation form follows from the PB formulation. Indeed, $\{H, H\} = 0$ implies that $\mathscr{E}_t = \{\mathscr{E}, H\}$ must be a divergence. The internal energy per unit volume is therefore

$$\rho\varepsilon_* = \rho\varepsilon + \frac{\beta_*}{2}\frac{(\nabla\rho)^2}{\rho}, \quad \text{where} \quad \varepsilon = \frac{p}{\rho(\gamma-1)} = \frac{T}{(\gamma-1)m}. \tag{9}$$

These regularization terms in the pressure, enthalpy, and internal energy depend upon density gradients and are therefore not strictly thermodynamic properties of the gas, any more than the regularized stress tensor. They are conservative analogs of the viscous stress tensor that depends on velocity gradients in dissipative gas dynamics.

Interestingly, the potential Φ in (5) is also the Bohm potential U[18] that arises as a correction to the classical potential V in the quantum-corrected Hamilton–Jacobi equation for the Schrödinger wavefunction $\psi = \sqrt{\rho}e^{iS/\hbar}$,

$$\rho_t + \nabla\cdot\left(\rho\frac{\nabla S}{m}\right) = 0 \quad \text{and} \quad S_t + \frac{(\nabla S)^2}{2m} + V + U = 0,$$

where

$$U = -\frac{\hbar^2}{2m}\frac{\nabla^2\sqrt{\rho}}{\sqrt{\rho}} = -\frac{\hbar^2}{4\,m}\left(\frac{\nabla^2\rho}{\rho} - \frac{1}{2}\frac{(\nabla\rho)^2}{\rho^2}\right). \tag{10}$$

Our regularized stress σ also resembles the Korteweg stress σ^{Kor} of Refs. 14 and 16. Indeed, if $\beta = \beta_*/\rho$,

$$\begin{aligned}\sigma^{\text{Kor}}_{ij} &= p\delta_{ij} - \rho[\partial_k(\beta(\rho)\partial_k\rho)]\delta_{ij} + \beta(\rho)\partial_i\rho\partial_j\rho\\ &= p\delta_{ij} - \beta_*\left[\left(\nabla^2\rho - \frac{1}{\rho}(\nabla\rho)^2\right)\delta_{ij} - \frac{\partial_i\rho\,\partial_j\rho}{\rho}\right].\end{aligned} \tag{11}$$

Although $\sigma_{ij}^{\mathrm{Kor}}$ has the term $(\beta_*/\rho)(\partial_i\rho)(\partial_j\rho)$ in common with σ_{ij} (6), they are not quite equal. Although the qualitative physical features of our equations may be similar to those of the Korteweg equations, our equations additionally possess some remarkable mathematical properties facilitating the analysis in this paper.

Finally, if the flow domain is all of $\mathbb{R}^3$, then β_* can be scaled out by defining $\mathbf{R} = \mathbf{r}/\sqrt{\beta_*}$ and $T = t/\sqrt{\beta_*}$, just as we may eliminate the dispersion coefficient in KdV on the whole real line. By contrast, in the presence of a characteristic length scale l, β_* *cannot* be scaled out and l/λ serves as a conservative analog of the Reynolds number.

A. Lagrangian formulation via Clebsch variables

To obtain a Lagrangian for R-gas dynamics, we use the Clebsch representation[26,27] $\mathbf{v} = \nabla\phi + (\lambda\nabla\mu + \alpha\nabla s)/\rho$. The PBs in (3) are recovered by postulating canonical PBs among Clebsch variables,

$$\{\rho(\mathbf{r}), \phi(\mathbf{r}')\} = \{\alpha(\mathbf{r}), s(\mathbf{r}')\} = \{\lambda(\mathbf{r}), \mu(\mathbf{r}')\} = \delta(\mathbf{r} - \mathbf{r}'). \quad (12)$$

The Hamiltonian density in terms of Clebsch variables is

$$\mathscr{H} = \frac{\rho}{2}\left(\nabla\phi + \frac{(\lambda\nabla\mu + \alpha\nabla s)}{\rho}\right)^2 + \rho\,\varepsilon(\rho, s) + \frac{\beta_*}{2}\frac{(\nabla\rho)^2}{\rho}, \quad (13)$$

where $\varepsilon(\rho, s)$ is the ideal specific internal energy (9). The EOM (5) follow as the Euler–Lagrange (EL) equations for the Bateman–Thellung[28,29] Lagrangian density linear in velocities[30] augmented by the density gradient energy,

$$\mathscr{L}_1 = \rho_t\phi + \lambda_t\mu + \alpha_t s - \mathscr{H}. \quad (14)$$

The EL equations for α and λ imply the advection of s and μ, while that for ϕ is the continuity equation and that for s and μ are the evolution equations $\alpha_t + \nabla\cdot(\alpha\mathbf{v}) = \rho T$ and $\lambda_t + \nabla\cdot(\lambda\mathbf{v}) = 0$. The regularization only affects the EL equation for ρ. Upon using $p = \rho^2\partial\varepsilon/\partial\rho$, it becomes the time-dependent Bernoulli equation for adiabatic R-gas dynamics,

$$\phi_t - \frac{\mathbf{v}^2}{2} + \mathbf{v}\cdot\nabla\phi + \varepsilon(\rho, s) + \frac{p}{\rho} - \beta_*\left(\frac{\nabla^2\rho}{\rho} - \frac{1}{2}\frac{(\nabla\rho)^2}{\rho^2}\right) = 0. \quad (15)$$

Using these, one obtains (5) for $\mathbf{v}$. There are, of course, related Lagrangians for the same EOM, e.g.,

$$\mathscr{L}_2 = -\rho\phi_t - \lambda\mu_t - \alpha s_t - \mathscr{H}$$

and

$$\mathscr{L}_3 = \rho\left(\frac{\mathbf{v}^2}{2} - \varepsilon\right) - \frac{\beta_*}{2}\frac{(\nabla\rho)^2}{\rho} + \phi(\rho_t + \nabla\cdot(\rho\mathbf{v})) - \lambda\frac{D\mu}{Dt} - \alpha\frac{Ds}{Dt}. \quad (16)$$

Thus, we may interpret ϕ, λ, and α as Lagrange multipliers enforcing the EOM for ρ, μ, and s.

III. FORMULATION OF ONE-DIMENSIONAL REGULARIZED GAS DYNAMICS

A. Hamiltonian and equations of motion

In what follows, we will primarily be interested in 1D adiabatic R-gas dynamics where ρ, s, and p are independent of two of the Cartesian coordinates and $\mathbf{v} = (u(x, t), 0, 0)$. The non-zero PBs (3) simplify as $\mathbf{w} = 0$: $\{u, u\} = 0$ and

$$\{u(x), s(y)\} = \frac{s'}{\rho}\delta(x - y) \quad \text{and} \quad \{\rho(x), u(y)\} = \partial_y\delta(x - y). \quad (17)$$

The total mass ($\int\rho dx$), entropy ($\int\rho s dx$), and more generally $\int\rho\Sigma(s)dx$ for any $\Sigma(s)$ are Casimirs of this algebra. As before, the dynamics is generated by a Hamiltonian that involves a capillary energy,

$$H = \int\left[\frac{1}{2}\rho u^2 + \frac{p}{\gamma - 1} + \frac{1}{2}\beta(\rho)\,\rho_x^2\right]dx, \quad (18)$$

where $\beta(\rho)$ will be chosen by requiring that the momentum equation be in conservation form. The continuity and entropy equations are as in the ideal model,

$$\rho_t + (\rho u)_x = 0, \quad s_t + u s_x = 0 \quad \text{with} \quad s = c_v\log\left(\frac{p\tilde{\rho}^\gamma}{\tilde{p}\rho^\gamma}\right). \quad (19)$$

Thus, even with our regularization, we continue to have $D_t p = c_s^2 D_t\rho$, where $c_s^2 = (\partial p/\partial\rho)_s = \gamma p/\rho$. The regularized momentum and velocity equations are

$$(\rho u)_t + (\rho u^2 + p)_x = \rho\left[(\beta\rho_x)_x - \frac{1}{2}\beta'\rho_x^2\right]_x$$

and

$$u_t + u u_x = -\frac{p_x}{\rho} + \left[(\beta\rho_x)_x - \frac{1}{2}\beta'\rho_x^2\right]_x. \quad (20)$$

The simplest way for the former to be in conservation form is for the momentum density to equal ρu and for the regularization term to be a divergence. $\beta = \beta_*/\rho$ is the simplest capillarity coefficient that ensures this, giving

$$(\rho u)_t + \left[\rho u^2 + p - \beta_*\left(\rho_{xx} - \frac{\rho_x^2}{\rho}\right)\right]_x = 0$$

and

$$\frac{Du}{Dt} + \frac{p_x}{\rho} = \beta_* f = \beta_*\left[\frac{\rho_{2x}}{\rho} - \frac{\rho_x^2}{2\rho^2}\right]_x = 2\beta_*\left[\frac{(\sqrt{\rho})_{xx}}{\sqrt{\rho}}\right]_x. \quad (21)$$

We note that the apparently simpler choice of constant β leads to a KdV-like ρ_{xxx} term in the velocity equation, but prevents the momentum equation from being in conservation form. Our regularization amounts to modifying the pressure $p \to p_*$ in the momentum and velocity equations

$$(\rho u)_t + (\rho u^2 + p_*)_x = 0 \quad \text{and} \quad u_t + u u_x = -\frac{{p_*}_x}{\rho},$$

where

$$p_* = p - \beta_*(\rho_{xx} - \rho_x^2/\rho). \quad (22)$$

It is instructive to compare our velocity equation with Korteweg's. For capillarity coefficient $\beta = \beta_*/\rho$, the 1D Korteweg velocity equation following from (11) is

$$u_t + u u_x + \frac{p_x}{\rho} = \beta_* f^{\mathrm{Kor}} = \frac{\beta_*}{\rho}\left(\rho_{xx} - \frac{2\rho_x^2}{\rho}\right)_x. \quad (23)$$

Unlike our force per unit mass $\beta_* f$ which is a gradient, $\beta_* f^{\rm Kor}$ is not. Thus, in the barotropic case of Sec. III B where $p_x/\rho = h_x$, our velocity equation (21) (but not Korteweg's) comes into conservation form as in ideal gas dynamics. Finally, our energy equation is also in local conservation form

$$\left(\frac{1}{2}\rho u^2 + \frac{p}{\gamma-1} + \frac{\beta_*}{2}\frac{\rho_x^2}{\rho}\right)_t + \left(\frac{1}{2}\rho u^2 u + \frac{\gamma}{\gamma-1}pu\right)_x + \beta_*\left(\frac{\rho_x}{\rho}(\rho u)_x - \rho u\left(\frac{\rho_x}{\rho}\right)_x - \frac{1}{2}\frac{u\rho_x^2}{\rho}\right)_x = 0. \tag{24}$$

It takes a compact form in terms of a regularized specific internal energy ε_* and enthalpy h_*,

$$\left(\frac{1}{2}\rho u^2 + \rho\varepsilon_*\right)_t + \left(\rho\left(\frac{1}{2}u^2 + h_*\right)u + \beta_* u_x\rho_x\right)_x = 0,$$

where

$$\rho\varepsilon_* = \frac{p}{\gamma-1} + \frac{\beta_*}{2}\frac{\rho_x^2}{\rho} \quad \text{and} \quad \rho h_* = \rho\varepsilon_* + p_*. \tag{25}$$

The internal energy equation may be interpreted as the 1st law of thermodynamics for adiabatic flow,

$$D_t\varepsilon_* + p_* D_t\left(\frac{1}{\rho}\right) + \frac{\beta_*}{\rho}(u_x\rho_x)_x = TD_t s = 0. \tag{26}$$

Evidently, the gas does work against the pressure p_* as well as a new type of reversible, non-dissipative work due to the regularization while ensuring that the specific entropy s is constant along the flow.

The action corresponding to (14) possesses three obvious symmetries: (a) constant shift in ϕ, (b) space translation, and (c) time translation, leading to the local conservation laws for mass (ρ), momentum (ρu), and energy ($\frac{1}{2}\rho u^2 + \rho\varepsilon_*$) densities [Eqs. (19), (21), and (24)]. In addition, under an infinitesimal Galilean boost ($t \to t$, $x \to x - ct$), the fields transform as

$$\delta\phi = c(t\phi_x - x), \quad \delta u = c(tu_x - 1), \quad \text{and} \quad \delta\Upsilon = ct\Upsilon_x$$

for

$$\Upsilon = \rho, \alpha, s, \lambda, \quad \text{and} \quad \mu, \tag{27}$$

leading to a change in the Lagrangian (16) by a spatial derivative $\delta\mathscr{L}_2 = ct(p - \beta_*\rho_{xx})_x$. The corresponding Noether charge and flux densities are

$$j^t = \sum_\chi \frac{\partial\mathscr{L}_2}{\partial\dot\chi}\delta\chi \quad \text{and} \quad j^x = \sum_\chi \frac{\partial\mathscr{L}_2}{\partial\chi_x}\delta\chi - ct(p - \beta_*\rho_{xx}). \tag{28}$$

Here, we sum over $\chi = \rho$, ϕ, α, s, λ, and μ. The resulting conservation law $\partial_t j^t + \partial_x j^x = 0$ or $(\rho(x-tu))_t + (x\rho u - tF^{\rm p})_x = 0$ involves an explicitly time-dependent Galilean charge and flux, where $F^{\rm p} = \rho u^2 + p - \beta_*\rho(\log\rho)_{xx}$ is the regularized momentum flux (21). Thus, $G = \int(x - tu)\rho dx$ is conserved even though $\{G, H\} = P$, where $P = \int\rho u dx$ is the total momentum. P, G, and H satisfy a 1D Galilei algebra with the total mass M furnishing a central extension: $\{G, P\} = M$.

B. Isentropic R-gas dynamics of a polytropic gas

Sans entropy sources/sinks and boundaries, one is mainly interested in cases where $s = \bar s$ is initially constant and by (19), independent of time. Thus, we consider isentropic flow where p and ρ satisfy the barotropic relation

$$p = (\gamma-1)K\rho^\gamma, \quad \text{where} \quad K = \frac{e^{\bar s/c_v}}{\gamma-1}\frac{\bar p}{\bar\rho^\gamma} > 0 \tag{29}$$

is a constant that encodes the constant value of entropy and labels isentopes. A feature of isentropic flow is that in addition to the continuity, momentum, and energy equations, the velocity equation is *also* in conservation form,

$$\rho_t + F^{\rm m}_x = 0, \quad (\rho u)_t + F^{\rm p}_x = 0, \quad \left[\frac{1}{2}\rho u^2 + \rho\varepsilon + \frac{\beta_*}{2}\frac{\rho_x^2}{\rho}\right]_t + F^{\rm e}_x = 0 \quad \text{and} \quad u_t + F^{\rm u}_x = 0. \tag{30}$$

Here, $\varepsilon = K\rho^{\gamma-1}$ and $h = \gamma K\rho^{\gamma-1}$ are specific internal energy and enthalpy, respectively. The corresponding fluxes are

$$F^{\rm m} = \rho u, \quad F^{\rm p} = \rho u^2 + p - \beta_*\left(\rho_{xx} - \frac{\rho_x^2}{\rho}\right),$$
$$F^{\rm e} = \left(\frac{u^2}{2} + h\right)\rho u + \beta_*\left(\frac{\rho_x}{\rho}(\rho u)_x - \rho u\left(\frac{\rho_x}{\rho}\right)_x - \frac{u\rho_x^2}{2\rho}\right),$$

and

$$F^{\rm u} = \frac{1}{2}u^2 + h - \beta_*\left(\frac{\rho_{xx}}{\rho} - \frac{1}{2}\frac{\rho_x^2}{\rho^2}\right). \tag{31}$$

In ideal gas dynamics, $F^{\rm u} = F^{\rm e}/F^{\rm m}$, but no such algebraic relation holds when $\beta_* \neq 0$. The emergence of a 4th conservation law in the isentropic case is tied to the global constancy of entropy. These equations follow from the degenerate Landau PBs $\{\rho, \rho\} = \{u, u\} = 0$ and $\{\rho(x), u(y)\} = \partial_y\delta(x-y)$ whose Casimirs include $M = \int\rho dx$ and $\int u dx$. These PBs become canonical [$\{\rho(x), \phi(y)\} = \delta(x-y)$] upon introducing a velocity potential $u(y) = \phi_y$. The corresponding EOM follow the Lagrangian $\mathscr{L}_1 = \rho_t\phi - \mathscr{H}$, where $\mathscr{H} = \frac{1}{2}\rho\phi_x^2 + \rho\varepsilon(\rho) + \frac{1}{2}\beta_*\rho_x^2/\rho$. As described above, the local conservation laws for mass, momentum, energy, and Galilei charge follow from Noether's theorem. However, the conservation law $u_t + F^{\rm u}_x = 0$ (30) does not arise from a symmetry via Noether's theorem. This is because $C = \int u dx$ is a Casimir, and it acts trivially on all observables: $\delta\phi = \{C, \phi\} = 0$.

IV. DISPERSIVE SOUND, STEADY AND TRAVELING WAVES

A. Dispersive sound waves

To discuss sound waves, it is convenient to nondimensionalize the variables in (19) and (22),

$$x = l\hat x, \quad t = \frac{l}{\bar c}\hat t, \quad \rho = \bar\rho\hat\rho, \quad p = \bar p\hat p, \quad \bar c^2 = \frac{\gamma\bar p}{\bar\rho},$$
$$u = \bar c\hat u, \quad \hat s = \frac{s}{c_v} = \log\left(\frac{\hat p}{\hat\rho^\gamma}\right). \tag{32}$$

Here, l is a macroscopic length. The nondimensional (hatted) variables satisfy

$$\hat{\rho}_{\hat{t}} + (\hat{\rho}\hat{u})_{\hat{x}} = 0, \quad \hat{s}_{\hat{t}} + \hat{u}\hat{s}_{\hat{x}} = 0,$$

and

$$\hat{u}_{\hat{t}} + \hat{u}\hat{u}_{\hat{x}} = -\frac{1}{\gamma}\frac{\hat{p}_{\hat{x}}}{\hat{\rho}} + \frac{\varepsilon^2}{\hat{\rho}}\left(\hat{\rho}_{\hat{x}\hat{x}} - \frac{\hat{\rho}_{\hat{x}}^2}{\hat{\rho}}\right)_{\hat{x}}. \tag{33}$$

Here, $\beta_* = \tilde{c}^2\lambda^2$, where λ is a regularization length and $\varepsilon = \lambda/l$ is its nondimensional version.

A homogeneous, stationary fluid ($\hat{\rho} = 1$, $\hat{p} = 1$, $\hat{u} = 0$, and $\hat{s} = 0$) is a solution of (33). To study sound, we consider linear perturbations $\hat{p} = 1 + \delta\tilde{p}$, $\hat{\rho} = 1 + \delta\tilde{\rho}$, $\hat{s} = \delta\tilde{s}$, and $\hat{u} = \delta\tilde{u}$ around this solution where $\delta \ll 1$. The entropy equation upon linearization gives $\tilde{s}_t = 0$. If we initially choose $\tilde{s}(x,0) \equiv 0$, then $\tilde{s}(x,t) \equiv 0$ and the entropy $\hat{s}(x,t) = \log(\hat{p}/\hat{\rho}^\gamma) = 0$. Linearizing this, we get $\tilde{p} = \gamma\tilde{\rho}$. The linearized continuity and velocity equations are

$$\tilde{\rho}_{\hat{t}} + \tilde{u}_{\hat{x}} = 0 \quad \text{and} \quad \tilde{u}_{\hat{t}} = -\tilde{\rho}_{\hat{x}} + \varepsilon^2\tilde{\rho}_{\hat{x}\hat{x}\hat{x}}. \tag{34}$$

Thus, we arrive at an equation for dispersive sound $\tilde{\rho}_{\hat{t}\hat{t}} = \tilde{\rho}_{\hat{x}\hat{x}} - \varepsilon^2\tilde{\rho}_{4\hat{x}}$. The 4th derivative is reminiscent of elasticity, so our regularization force is like a tension. Figure 1 shows the splitting of a pulse in density into two smaller pulses including the effects of dispersion and weak nonlinearity. Equations (34) have several conserved quantities including

$$M = \int \tilde{\rho}\, d\hat{x}, \quad P = \int \tilde{u}\, d\hat{x}, \quad H_1 = \frac{1}{2}\int [\tilde{u}^2 + \tilde{\rho}^2 + \varepsilon^2\tilde{\rho}_{\hat{x}}^2]d\hat{x},$$

and

$$H_2 = \frac{1}{2}\int \left[\tilde{\rho}_{\hat{t}}^2 + \tilde{\rho}_{\hat{x}}^2 + \varepsilon^2\rho_{\hat{x}\hat{x}}^2\right]d\hat{x}. \tag{35}$$

Putting $\tilde{\rho} \propto e^{i(k\hat{x}-\omega\hat{t})}$, we get a dispersion relation akin to that of linearized KdV ($u_t + uu_x = \varepsilon u_{3x}$), $\omega_{\text{KdV}} = k + \varepsilon k^3$,

$$\omega^2 = k^2(1+\varepsilon^2k^2) \text{ or } \omega = \pm\left(k + \frac{1}{2}\varepsilon^2k^3 + \cdots\right). \tag{36}$$

The phase velocity is $v_p = \omega/k = \pm(1+\varepsilon^2k^2)^{1/2} \approx \pm(1+\frac{1}{2}\varepsilon^2k^2)$, while the group velocity is

$$v_g = \frac{\partial\omega}{\partial k} = \pm\frac{1+2\varepsilon^2k^2}{\sqrt{(1+\varepsilon^2k^2)}} \approx \pm(1+2\varepsilon^2k^2)(1-\frac{1}{2}\varepsilon^2k^2+\ldots)$$
$$= \pm\left(1+\frac{3}{2}\varepsilon^2k^2+\cdots\right). \tag{37}$$

Note that the regularization increases the phase speed while $|v_g|$ always exceeds $|v_p|$.

B. Steady and traveling waves in one-dimension

Traveling waves are those where ρ, u, p, and s are functions only of $(x - ct)$, where c is the velocity of the wave. The entropy equation $s_t + us_x = 0$ becomes $(u - c)\, s' = 0$. Thus, either $s = \bar{s}$ is a constant in space and time or $u = c$. In the former case, we have isentropic flow. In the latter, s can be an arbitrary function of $(x - ct)$, but the fluid is at rest ("aerostatic") in a frame moving at velocity c. We will focus on the first possibility and look at steady solutions, subsequently "boosting" them to get traveling waves.

1. Isentropic steady solutions

For steady flow ($c = 0$), the mass, momentum, and velocity fluxes (31) are constant. Moreover, the steady continuity equation $u\rho_x + u_x\rho = 0$ implies that the constant energy flux of Eq. (31) is not independent: $F^{\text{e}} = F^{\text{m}}F^{\text{u}}$. Eliminating $u = F^{\text{m}}/\rho$, we get two expressions for ρ_{xx},

$$\beta_*\rho_{xx} = -F^{\text{p}} + \frac{(F^{\text{m}})^2}{\rho} + (\gamma-1)K\rho^\gamma + \beta_*\frac{\rho_x^2}{\rho}$$

and

$$\beta_*\rho_{xx} = -F^{\text{u}}\rho + \frac{(F^{\text{m}})^2}{2\rho} + \gamma K\rho^\gamma + \frac{\beta_*}{2}\frac{\rho_x^2}{\rho}. \tag{38}$$

Taking a linear combination allows us to eliminate the ρ^γ term and arrive at the second order equation

$$\beta_*\rho_{xx} = -V'(\rho) + \frac{(\gamma+1)\beta_*}{2}\frac{\rho_x^2}{\rho},$$

where

$$V'(\rho) = F^{\text{p}}\gamma - F^{\text{u}}(\gamma-1)\rho - \frac{(\gamma+1)(F^{\text{m}})^2}{2\rho}. \tag{39}$$

In Appendix C, a different linear combination that eliminates the ρ_x^2/ρ term is considered, leading to additional results. The current choice makes it easier to treat all values of γ in a uniform manner. Interpreting x and ρ as time and position, this describes a Newtonian particle of mass β_* moving in a (linear + harmonic + logarithmic) potential V on the positive half-line subject also to a "velocity-dependent" force $\propto \rho_x^2/\rho$. This ensures that the motion is "time-reversal' ($x \to -x$) invariant. The qualitative nature of trajectories is elucidated via a ρ–ρ_x phase plane analysis in

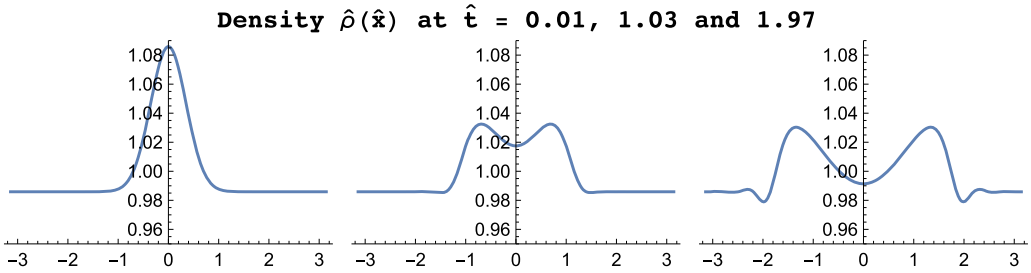

FIG. 1. R-gas dynamic evolution of a pulse [$\hat{\rho}(\hat{x},0) = 1 + 0.1e^{-4\hat{x}^2}$ and $\hat{u}(\hat{x},0) = 0$] showing d'Alembert-like splitting of the pulse. Dispersion and nonlinearity modify the shape and produce "forerunners" and "backrunners." The evolution is for $\gamma = 2$ and $\varepsilon = 0.1$ with periodic BCs using the scheme of Sec. VI with $n_{\text{max}} = 20$ Fourier modes, a time step $\Delta = 0.01$, and "nonlinearity strength" $\delta = 0.1$.

Appendix A. There are only two types of non-constant bounded solutions for $\rho(x)$: solitary waves of depression (cavitons) and periodic waves. The latter correspond to closed trajectories around an elliptic fixed point (O-point) in the phase portrait, while cavitons correspond to the homoclinic separatrix orbit that encircles an O-point and begins and ends at a hyperbolic X-point to its right. The location of these fixed points is determined (for any γ) by the roots of the quadratic $V'(\rho) = 0$ whose discriminant $\Delta = \gamma^2(F^{\rm p})^2 - 2(\gamma^2 - 1)F^{\rm u}(F^{\rm m})^2$ must therefore be positive. In the generic non-aerostatic situation (i.e., $u \not\equiv 0$ or equivalently $F^{\rm m} \neq 0$), the only cases when we get non-constant bounded solutions for ρ are (a) $F^{\rm p}$, $F^{\rm u} > 0$: both periodic solutions and cavitons and (b) $F^{\rm u} < 0$: only periodic solutions.

Remark. Equation (39) is a generalization of the Ermakov–Pinney equation,[31,32] which corresponds to $V(\rho) = \rho^4/2$, $\gamma = 2$, and $\beta_* = 1$. This leads to an alternate approach to understanding (39), since the transformation $z^2 = 1/\rho$ converts it into a Newton equation with sextic potential and no velocity dependent force for any γ,

$$z_{xx} = \frac{1}{2}(\gamma - 1)F^{\rm u}z - \gamma F^{\rm p}z^3 + \frac{(\gamma+1)}{4(F^{\rm m})^2}z^5. \tag{40}$$

Reduction to quadrature: Subtracting the two equations in (38), we get a first order ordinary differential equation (ODE) for ρ,

$$\frac{\beta_*}{2}\rho_x^2 = -\frac{(F^{\rm m})^2}{2} + F^{\rm p}\rho - F^{\rm u}\rho^2 + K\rho^{\gamma+1} \equiv \rho^{\gamma+1}(K - U),$$

where

$$K = \frac{1}{2}\left(\frac{\beta_*}{\rho^{\gamma+1}}\right)\rho_x^2 + U$$

and

$$U(\rho) = \frac{1}{\rho^{\gamma+1}}\left[\frac{(F^{\rm m})^2}{2} - F^{\rm p}\rho + F^{\rm u}\rho^2\right]. \tag{41}$$

The "potential energy" U is related to the potential V via $\rho^{\gamma+1}U'(\rho) = V'(\rho)$. This allows us to reduce the determination of the steady density profile $\rho(x)$ to quadrature,

$$dx = \frac{d\rho}{\sqrt{(2/\beta_*)\rho^{\gamma+1}(K - U(\rho))}} = \frac{d\rho}{\sqrt{(2/\beta_*)(K\rho^{\gamma+1} - F^{\rm u}\rho^2 + F^{\rm p}\rho - ((F^{\rm m})^2/2))}}. \tag{42}$$

For integer $\gamma \geq 1$, (42) is a hyperelliptic integral though it reduces to an elliptic integral when $\gamma = 2$ (see Sec. IV B 3). For other values of γ, steady solutions may be found via the parabolic embedding of Appendix C.

2. Nondimensionalizing the steady equation

To integrate (41), it is convenient to replace the four constants ($F^{\rm m}$, $F^{\rm p}$, $F^{\rm u}$, K) with two dimensionless shape parameters ($\kappa_\circ$, $M_\circ$) and two dimensional ones ($\rho_\circ$, $c_\circ$) that set scales. These parameters are adapted to the solutions one seeks to find: $\rho_\circ$ is the density at a point $x_\circ$ where $\rho_x = 0$. For a caviton, $\rho_\circ$ can be the asymptotic or trough density, while for a periodic wave, it can be the trough or crest density (or the trough density of an unbounded solution with the same K). This choice will simplify the expressions for the constant fluxes (31) and K when evaluated at $x_\circ$. For example, $K = U(\rho_\circ)$ gives

$$K = \frac{1}{\rho_\circ^{\gamma+1}}\left[\frac{(F_\circ^{\rm m})^2}{2} - F_\circ^{\rm p}\rho_\circ + F_\circ^{\rm u}\rho_\circ^2\right] = \frac{p_\circ\rho_\circ^{-\gamma}}{\gamma - 1} = \frac{c_\circ^2\rho_\circ^{1-\gamma}}{\gamma(\gamma-1)}, \tag{43}$$

where $p_\circ$ and $c_\circ$ are the pressure and sound speed at $x_\circ$. We may use $c_\circ^2$ to trade β_* for a regularization length $\lambda_\circ = \sqrt{\beta_*}/c_\circ$, which is used to define the nondimensional position $\xi = x/\lambda_\circ$. Next, let $M_\circ^2 = u_\circ^2/c_\circ^2$ be the square of the Mach number at $x_\circ$. Positive $M_\circ$ corresponds to rightward flow at $x_\circ$ and vice versa. We will take $M_\circ \geq 0$ with the remaining steady solutions obtained by taking $M_\circ \to -M_\circ$. Using these definitions, we rewrite (41) as a 1st order ODE for the nondimensional density $\tilde\rho(\xi) = \rho(\lambda_\circ\xi)/\rho_\circ$,

$$\frac{1}{2}\left(\frac{d\tilde\rho}{d\xi}\right)^2 = \mathscr{T}(\tilde\rho) \equiv \frac{\tilde\rho^{\gamma+1}}{\gamma(\gamma-1)} - \frac{M_\circ^2}{2}(\tilde\rho - 1)^2 - \frac{\tilde\rho^2}{\gamma - 1} - \kappa_\circ\tilde\rho(1 - \tilde\rho) + \frac{\tilde\rho}{\gamma}. \tag{44}$$

Here, $\kappa_\circ = \lambda_\circ^2\rho''(x_\circ)/\rho_\circ = \tilde\rho''(\xi_\circ)$ measures the curvature of the density profile at $x_\circ = \lambda_\circ\xi_\circ$. A virtue of this nondimensionalization is that unlike the four parameters in (41), only two parameters $\kappa_\circ$ and $M_\circ$ appear in (44). Equation (44) describes zero energy trajectories $\tilde\rho(\xi)$ of a unit mass particle in the potential $-\mathscr{T}(\tilde\rho)$. Evidently, the allowed values of $\tilde\rho$ must lie between adjacent positive zeros of $\mathscr{T}$ with $\mathscr{T} > 0$ in between (Fig. 2). To obtain (44), we used the following expressions for the constant fluxes and entropy:

$$(F^{\rm m})^2 = \rho_\circ^2 c_\circ^2 M_\circ^2, \quad F^{\rm p} = \rho_\circ c_\circ^2\left(M_\circ^2 + \frac{1}{\gamma} - \kappa_\circ\right), \quad F^{\rm u} = c_\circ^2\left(\frac{M_\circ^2}{2} + \frac{1}{\gamma - 1} - \kappa_\circ\right), \quad \text{and} \quad K = \frac{c_\circ^2\rho_\circ^{1-\gamma}}{\gamma(\gamma-1)}. \tag{45}$$

Conversely, we may invert (45) by first determining $\rho_\circ$ by solving the algebraic equation following from (41):

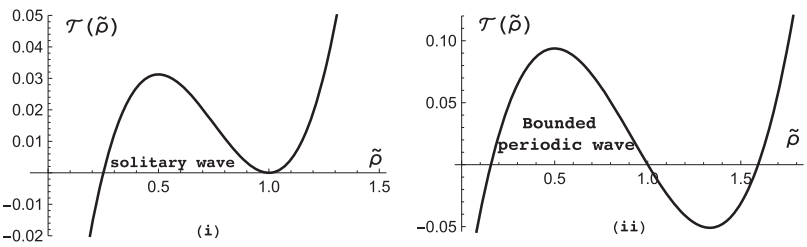

FIG. 2. (i) Density of the caviton lies between simple and double root of $\mathscr{T}(\tilde\rho)$ (44). (ii) Periodic wave density lies between simple roots where $\mathscr{T} > 0$. Here, $\gamma = 2$ and in (i) $\kappa_\circ = 0$, $M_\circ = 0.5$, while in (ii) $\kappa_\circ = -0.25$ and $M_\circ = 0.5$.

$$K = U(\rho_\circ) = \rho_\circ^{-(1+\gamma)}\left[\frac{(F^{\mathrm{m}})^2}{2} - F^{\mathrm{p}}\rho_\circ + F^{\mathrm{u}}\rho_\circ^2\right]. \tag{46}$$

The remaining new parameters follow from (45) and (31),

$$\frac{c_\circ^2}{\gamma} = \frac{K(\gamma-1)}{\rho_\circ^{1-\gamma}}, \quad M_\circ^2 = \frac{(F^{\mathrm{m}})^2}{\rho_\circ^2 c_\circ^2}, \quad \kappa_\circ = \frac{(F^{\mathrm{m}})^2 - \rho_\circ F^{\mathrm{p}}}{\rho_\circ^2 c_\circ^2} + \frac{1}{\gamma}. \tag{47}$$

3. Exact cavitons and cnoidal waves for $\gamma = 2$

For $\gamma = 2$, $\mathscr{T}(\tilde\rho)$ (44) becomes cubic with roots $\tilde\rho = 1$ and

$$\tilde\rho_\pm = \frac{1}{2}\left(1 + M_\circ^2 - 2\kappa_\circ \pm \sqrt{(1+M_\circ^2-2\kappa_\circ)^2 - 4M_\circ^2}\right). \tag{48}$$

The density of periodic and solitary waves must lie between adjacent positive roots with $\mathscr{T} > 0$ in between. Interestingly, it can be shown that if for $\gamma = 2$, all three roots of $\mathscr{T}$ are positive, then the same holds for any $1 < \gamma < 2$. So some qualitative features of solutions for $\gamma = 2$ are valid more generally. For $\gamma = 2$, the nature of solutions on the $\kappa_\circ$–$M_\circ$ plane [Fig. 3(a)] changes when the two relevant roots coalesce, i.e., when the discriminant of the cubic $\mathscr{T}$ vanishes,

$$\begin{aligned}\Delta(\kappa_\circ, M_\circ) &= [(\tilde\rho_+ - \tilde\rho_-)(\tilde\rho_- - 1)(1-\tilde\rho_+)]^2 \\ &= 4\kappa_\circ^2\left[M_\circ^4 - 2M_\circ^2(1+2\kappa_\circ) + (1-2\kappa_\circ)^2\right] = 0.\end{aligned} \tag{49}$$

Δ vanishes only along the vertical axis $\kappa_\circ = 0$, the two parabolic curves $M_\circ = 1 \pm \sqrt{2\kappa_\circ}$, and their reflections in the $\kappa_\circ$-axis. In what follows, we restrict to rightward flow by taking $M_\circ \geq 0$. There are three regions in the upper half $\kappa_\circ$–$M_\circ$ plane [see Fig. 3(a)] admitting *periodic solutions*: (a) the blue second quadrant $\kappa_\circ < 0$, (b) the red north-east region above $M_\circ = 1 + \sqrt{2\kappa_\circ}$, and (c) the yellow triangular region below the curve $M_\circ = 1 - \sqrt{2\kappa_\circ}$. In the green wedge (d) lying within the parabola but above the horizontal axis, non-constant solutions are unbounded since $\tilde\rho_\pm$ are either negative (when $M_\circ < -1 + \sqrt{2\kappa_\circ}$) or not real (when $M_\circ > -1 + \sqrt{2\kappa_\circ}$).

Solitary waves (cavitons) occur only on the dashed boundaries (i) between (a) and (c) ($0 < M_\circ < 1$, $\kappa_\circ = 0$) and (ii) between (b) and (d) ($M_\circ = 1 + \sqrt{2\kappa_\circ}$). When $\kappa_\circ = M_\circ = 0$, $\mathscr{T} = \tilde\rho(\tilde\rho - 1)^2/2$ so that we have an aerostatic ($u \equiv 0$) caviton with $0 \leq \tilde\rho \leq 1$. *Constant solutions* occur when $\tilde\rho \equiv$ any zero of $\mathscr{T}$. $\mathscr{T}$ has a double zero ($\tilde\rho = 1$) along the vertical axis, the double zero $\tilde\rho_+ = \tilde\rho_-$ along the curve $M_\circ = 1 - \sqrt{2\kappa_\circ}$, and the triple zero $\tilde\rho = 1$ at ($\kappa_\circ = 0$, $M_\circ = 1$). At all other points, $\mathscr{T}$ has either one or three positive simple zeros.

Interestingly, when we reinstate dimensions, the periodic solutions from regions (a), (b), and (c) of the $\kappa_\circ$–$M_\circ$ plane [Fig. 3(a)] are physically identical. They differ by the choice of nondimensionalizing density $\rho_\circ$ that could be any one of the roots of the cubic in (46). Thus, the parameters ($\kappa_\circ$, $M_\circ$, $c_\circ$, $\rho_\circ$) generically furnish a 3-fold cover (redundancy) of the original space of constants $((F^{\mathrm{m}})^2, F^{\mathrm{u}}, F^{\mathrm{p}}, K)$. For solitary waves, it degenerates into a double cover: the two families of cavitons [(i) and (ii)] in Fig. 3(a) differ via the choice of $\rho_\circ$ as trough or asymptotic density. Moreover, $M_\circ$ is the Mach number at the trough in (i), while it is the asymptotic Mach number in (ii). In a caviton, the flow goes from asymptotically subsonic to supersonic at $x = 0$. A caviton is like a pair of normal shocks joined at the trough. Finally, the map between the two sets of parameters becomes a 1-fold cover for the aerostatic cavitons at $\kappa_\circ = M_\circ = 0$, since their trough densities vanish and $\rho_\circ$ can only be chosen as the asymptotic density.

In light of the above remarks, we now restrict our attention to the yellow triangular region (c) where $\kappa_\circ > 0$ and $0 < M_\circ < 1 - \sqrt{2\kappa_\circ}$. Here, the roots of $\mathscr{T}$ are $0 < \tilde\rho_- < \tilde\rho_+ < 1$, and (44) is reduced to quadrature,

$$\begin{aligned}\xi(\tilde\rho) - \xi(\tilde\rho_-) &= \int_{\tilde\rho_-}^{\tilde\rho} \frac{d\rho'}{\sqrt{(\rho'-\tilde\rho_-)(\rho'-\tilde\rho_+)(\rho'-1)}} \\ &= \frac{2}{\sqrt{1-\tilde\rho_-}} F\left(\arcsin\sqrt{\frac{\tilde\rho-\tilde\rho_-}{\tilde\rho_+-\tilde\rho_-}} \,\middle|\, \frac{\tilde\rho_+-\tilde\rho_-}{1-\tilde\rho_-}\right).\end{aligned} \tag{50}$$

Here, $F(\phi|m) = \int_0^\phi (1 - m\sin^2\theta)^{-1/2} d\theta$ is the incomplete elliptic integral of the first kind with m being the square of the elliptic modulus k (see 17.4.62 of Ref. 33). Inverting, we write $\tilde\rho(\xi)$ in terms of the Jacobi $\mathrm{cn}(u, m)$ function,

$$\tilde\rho(\xi) = \tilde\rho_+ - (\tilde\rho_+ - \tilde\rho_-)\ \mathrm{cn}^2\left(\frac{\sqrt{1-\tilde\rho_-}}{2}(\xi - \xi_-), \frac{\tilde\rho_+-\tilde\rho_-}{1-\tilde\rho_-}\right). \tag{51}$$

Here, $\xi_- = \xi(\tilde\rho_-)$. The periodic wave extends from a trough at $\tilde\rho_-$ to a crest at $\tilde\rho_+$ with amplitude and wavelength,

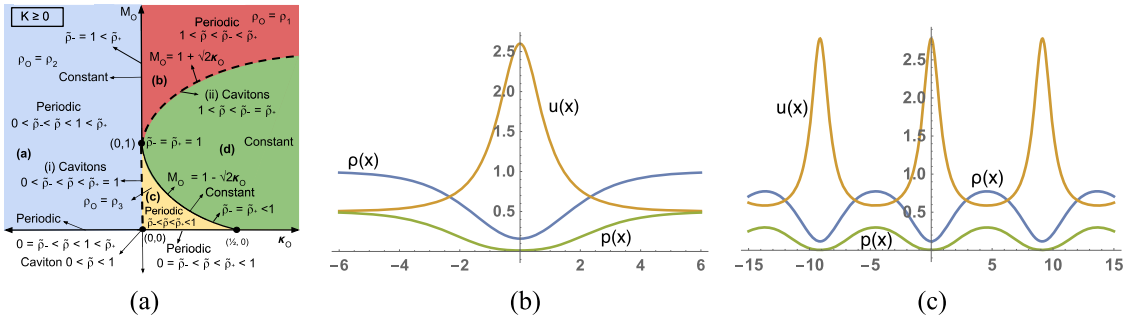

FIG. 3. (a) Nature of steady bounded solutions (44) for $\gamma = 2$ in the $\kappa_\circ$-$M_\circ$ parameter space. [(b) and (c)] Density, velocity, and pressure for $K = 1/2$ for (b) traveling cavitons ($\rho_\circ = c_\circ = 1$, $M_\circ = 0.5$, $\kappa = 0$, and $\tilde c = 0.1$) and (c) traveling periodic cnoidal waves $\rho_\circ = c_\circ = 1$, $M_\circ = 0.5$, $\kappa = 0.1$, and $\tilde c = 0.2$ (lower triangular region in the $|M_\circ - \tilde c|$–$\kappa_\circ$ plane). Cavitons are solutions where the temperature drops isentropically in a small region of size $\lambda_\circ$.

$$\mathscr{A}_{\kappa_\circ>0} = \sqrt{(1+M_\circ^2-2\kappa_\circ)^2-4M_\circ^2}$$

and

$$\Lambda_{\kappa_\circ>0} = \int_{\tilde\rho_-}^{\tilde\rho_+} \frac{2\,d\tilde\rho}{\sqrt{2\mathscr{T}(\tilde\rho)}} = \frac{4}{\sqrt{1-\tilde\rho_-}} K\left(\frac{\tilde\rho_+-\tilde\rho_-}{1-\tilde\rho_-}\right). \tag{52}$$

Here, $K(m) = F(\frac{\pi}{2}|m)$ is the complete elliptic integral of the 1st kind. When we approach the left boundary $\kappa_\circ \to 0^+$ with $0 < M_\circ < 1$, the wavelength diverges ($K(1/2\kappa_\circ) \sim \sqrt{\kappa_\circ}\log\kappa_\circ$ for small $\kappa_\circ$) and the periodic waves turn into cavitons that extend from a trough density $\tilde\rho = \tilde\rho_- = M_\circ^2 < 1$ to an asymptotic density $\tilde\rho = \tilde\rho_+ = 1$,

$$\tilde\rho(\xi) = 1-(1-M_\circ^2)\,\mathrm{sech}^2\left(\sqrt{\frac{1-M_\circ^2}{4}}\xi\right) \quad \text{for} \quad 0 \le M_\circ \le 1. \tag{53}$$

On the other hand, when we approach the upper boundary $M_\circ = 1-\sqrt{2\kappa_\circ}$, $\mathscr{A}\to 0$ and we get constant solutions. By contrast, on the lower boundary ($M_\circ = 0, 0 < \kappa_\circ < \frac{1}{2}$), we continue to have periodic solutions except that $\tilde\rho$ vanishes at the trough ($\tilde\rho_- = 0$) while the crest density $\tilde\rho_+ = 1-2\kappa_\circ$,

$$\tilde\rho(\xi) = (1-2\kappa_\circ)\,\mathrm{sn}^2\left(\frac{\xi}{2}, 1-2\kappa_\circ\right)$$

and

$$\Lambda = 2i\left[\sqrt{\frac{2}{\kappa_\circ}}K\left(\frac{1}{2\kappa_\circ}\right) - 2\,K(2\kappa_\circ)\right]. \tag{54}$$

When $\kappa_\circ = M_\circ = 0$ in (53) or (54), we get an *aerostatic caviton* that reaches *vacuum conditions* at $\xi = 0$,

$$\tilde\rho(\xi) = \tanh^2(\xi/2) \quad \text{with} \quad u \equiv 0. \tag{55}$$

The dimensional ρ, u, and p are got by reinstating the constants $\lambda_\circ$, $\rho_\circ$, and $c_\circ$. Writing $x = \lambda_\circ\xi$, we have

$$\rho(x) = \rho_\circ\tilde\rho(\xi),\ u(x) = \frac{c_\circ M_\circ}{\tilde\rho(\xi)} \quad \text{and} \quad p(x) = \frac{c_\circ^2\rho_\circ}{\gamma}\tilde\rho(\xi)^\gamma \tag{56}$$

for isentropic flow. Reversing the sign of $M_\circ$ reverses the flow direction leaving p and ρ unaltered. Moreover, since $\tilde\rho \ge 0$ and $u = F^{\mathrm{m}}/\rho$, the flow is unidirectional with positive velocity solitary waves being waves of elevation in u and vice versa. A caviton is superficially a bifurcation of the constant solution $\rho(x) \equiv \rho(\pm\infty)$. Although the caviton and constant solutions have the same constant specific entropy, they have different values of mass and energy (per unit length). For instance, the energy density (18) of an aerostatic caviton is less than that of the constant state,

$$\mathscr{E}_{\text{aerostat cav}} = p_\infty\left[1-\frac{2\rho}{\rho_\infty}\left(1-\frac{\rho}{\rho_\infty}\right)\right] < \mathscr{E}_{\text{const.}} = p_\infty. \tag{57}$$

As a consequence, the uniform state cannot, by any isentropic time-dependent motion with fixed BCs at $\pm\infty$, in the absence of sources and sinks, evolve via R-gas dynamics to the caviton, or vice versa, since the two states have different invariants. However, one could imagine creating, say, an aerostatic caviton, by starting with a uniform state and introducing a point sink at the origin, to suck fluid out. A symmetrical pair of expansion waves would travel to infinity on both sides without affecting the conditions at infinity. When the density reaches 0 at the origin, we stop the sink. The pressure gradient will then be balanced by the regularizing density gradient force, and the solution should tend to the aerostatic caviton as $t\to\infty$. Since temperature $T = Km(\gamma-1)\rho^{\gamma-1}$, the caviton corresponds to a region of width λ where the temperature drops. Loosely, the regularizing force is like Pauli's exchange repulsion, capable of maintaining a depression in density with variable but isentropic temperature and pressure distributions.

4. Traveling waves of isentropic R-gas dynamics

Here, we generalize the above steady solutions to waves traveling at speed c: $(\rho, u, p)(x, t) = (\rho, u, p)(x-ct)$. The continuity, velocity, and momentum equations (30) are readily integrated, giving the constant fluxes,

$$F^{\mathrm{m}} = \rho(u-c),\quad F^{\mathrm{u}} = \frac{u^2}{2} - cu - \beta_*\left[\frac{\rho''}{\rho} - \frac{\rho'^2}{2\rho^2}\right] + \gamma K\rho^{\gamma-1}$$

and

$$F^{\mathrm{p}} = \rho u(u-c) + (\gamma-1)K\rho^\gamma - \beta_*\left(\rho'' - \frac{\rho'^2}{\rho}\right). \tag{58}$$

Eliminating $u = c + F^{\mathrm{m}}/\rho$ and taking a linear combination leads us to a 2nd order nonlinear ODE for ρ,

$$\beta_*\rho'' = -V'(\rho) + \frac{(\gamma+1)\beta_*}{2}\frac{\rho'^2}{\rho},$$

where

$$V'(\rho) = \gamma(cF^{\mathrm{m}} - F^{\mathrm{p}}) - (\gamma-1)\left(\frac{cF^{\mathrm{p}}}{F^{\mathrm{m}}} - F^{\mathrm{u}} - \frac{c^2}{2}\right)\rho + \frac{(\gamma+1)(F^{\mathrm{m}})^2}{2\rho}. \tag{59}$$

Proceeding as in Secs. IV B 1 and IV B 2, this may be reduced to the nonlinear first order equation

$$\frac{1}{2}\left(\frac{d\tilde\rho}{d\xi}\right)^2 = \mathscr{T}(\tilde\rho) \equiv \frac{\tilde\rho^{\gamma+1}}{\gamma(\gamma-1)} - \frac{1}{2}(\tilde\rho-1)^2(\tilde c - M_\circ)^2 - \frac{\tilde\rho^2}{\gamma-1} + \frac{\tilde\rho}{\gamma} - \kappa_\circ\tilde\rho(1-\tilde\rho),$$

where

$$\beta_* = \lambda_\circ^2 c_\circ^2,\quad \tilde\rho = \frac{\rho}{\rho_\circ},\quad \tilde c = \frac{c}{c_\circ},\quad M_\circ = \frac{u_\circ}{c_\circ},$$
$$\kappa_\circ = \tilde\rho''(\xi_\circ),\quad \text{and}\quad \xi = \frac{x-ct}{\lambda_\circ}\quad \text{with}\quad \tilde\rho'(\xi_0) = 0. \tag{60}$$

Comparing with (44), we see that the passage from steady to traveling waves involves only a shift in the square of the Mach number $M_\circ^2 \to (M_\circ - \tilde c)^2$. Here, $\tilde c$ is the speed of the traveling wave in units of the sound speed $c_\circ$ at the point where $\rho'(x-ct) = 0$. Thus, for each value of β_*, we have a 5-parameter $(\kappa_\circ, M_\circ, \rho_\circ, c_\circ, \tilde c)$ space of traveling cavitons and periodic waves. The dimensionful ρ, u, and p for any value of $(M_\circ - \tilde c)$ are given by

$$\rho(x,t) = \rho_\circ\tilde\rho(\xi),\quad u(x,t) = c_\circ\left(\frac{M_\circ-\tilde c}{\tilde\rho(\xi)} + \tilde c\right),$$

and

$$p(x,t) = \frac{c_\circ^2 \rho_\circ}{\gamma}\tilde{p}(\xi)^\gamma, \quad \text{where} \quad \xi = \frac{x - \tilde{c}\, c_\circ t}{\lambda_\circ}. \tag{61}$$

Traveling cavitons for $\gamma = 2$: In these nondimensional variables, traveling cavitons have the profile

$$\tilde{p}(\xi) = 1 - (1 - (\tilde{c} - M_\circ)^2)\,\mathrm{sech}^2\left(\sqrt{\frac{1 - (\tilde{c} - M_\circ)^2}{4}}\,\xi\right) \tag{62}$$

for $(\tilde{c} - M_\circ)^2 < 1$. These cavitons are reminiscent of the solitary waves of depression/elevation of the KdV equation $u_t \mp 6uu_x + u_{xxx} = 0$ that move rightward with speed $c > 0$: $u(x,t) = \mp(c/2)\,\mathrm{sech}^2\left((\sqrt{c}/2)(x - ct)\right)$. Just as in KdV, narrower cavitons (width $\propto 1/\sqrt{|\tilde{c} - M_\circ| - 1}$) are taller (height $\propto |\tilde{c} - M_\circ| - 1$) and have a higher speed relative to the speed at the reference location where the density has an extremum ($\tilde{c} - M_\circ \propto c - u_\circ$ is the speed of the traveling wave in the rest frame of the fluid at the reference location).

Traveling cnoidal waves for $\gamma = 2$: The nondimensional density profile of traveling cnoidal waves is

$$\tilde{\rho}(\xi) = \tilde{\rho}_+ - (\tilde{\rho}_+ - \tilde{\rho}_-)\,\mathrm{cn}^2\left(\frac{\sqrt{1 - \tilde{\rho}_-}}{2}(\xi - \xi_-), \frac{\tilde{\rho}_+ - \tilde{\rho}_-}{1 - \tilde{\rho}_-}\right)$$

for

$$0 < \kappa_\circ < \frac{1}{2} \quad \text{and} \quad |M_\circ - \tilde{c}| < 1 - \sqrt{2\kappa_\circ}. \tag{63}$$

Here, $\tilde{\rho}_\pm$ are got by replacing $M_\circ^2 \to (M_\circ - \tilde{c})^2$ in (48). Their wavelength is given by the same formula (52). Our cnoidal waves are very similar to those of KdV ($u_t - 6uu_x + u_{xxx} = 0$),

$$u = f(\xi) = f_2\left[1 - \mathrm{cn}^2\left[\sqrt{\frac{f_1 - f_2}{2}}(\xi - \xi_3), \frac{f_2 - f_3}{f_1 - f_3}\right]\right] + f_3. \tag{64}$$

Here, $\xi = x - ct$ and $f(\xi_3) = f_3$ and $f_{1,2,3}$ are the roots of $f^3 + \frac{1}{2}cf^2 + Af + B$ with A and B being constants of integration.

V. WEAK FORM AND SHOCK-LIKE PROFILES

A. Weak form of R-gas dynamic equations

The R-gas dynamic equations [(19) and (21)] involve u_x, p_x, ρ_x, ρ_{xx}, and ρ_{xxx}. Thus, classical solutions need to be C^1 in u and p and C^3 in ρ. However, by multiplying the conservation equations by C^∞ test functions ϕ, ψ, and ζ and integrating by parts, we arrive at a weak form of the equations

$$\int [\rho_t \phi - (\rho u)\phi_x]dx = 0,$$

$$\int \left[(\rho u)_t \psi - \left(p + \rho u^2 + \beta_* \frac{\rho_x^2}{\rho}\right)\psi_x + \beta_* \rho \psi_{xxx}\right]dx = 0,$$

and

$$\int \left[\frac{\rho u^2}{2} + \frac{p}{\gamma - 1} + \frac{\beta_* \rho_x^2}{2\rho}\right]_t \zeta dx = \int \left[\left[\frac{\rho u^3}{2} + \frac{\gamma p u}{\gamma - 1} + \frac{3\,\beta_*\, u}{2}\frac{\rho_x^2}{\rho}\right]\zeta_x - \beta_* u \rho_x \zeta_{xx}\right]dx. \tag{65}$$

Thus, for weak solutions, it suffices that ρ be C^1 and u and p be merely continuous.

B. Steady shock-like profile from half a caviton

Here, we try to use the steady solutions of Sec. IV B to model the structure of a normal shock propagating to the right in the lab frame. As in Fig. 4, in the shock frame, the shock is assumed to be located around $x = 0$. The undisturbed pre-shock medium is to the right ($x > 0$), while the "disturbed" post-shock medium is to the left ($x < 0$).[1] As $x \to \pm\infty$, the variables approach the asymptotic values $\rho_{\pm\infty}$, $u_{\pm\infty}$, and $p_{\pm\infty}$ with $\rho_{+\infty} < \rho_{-\infty}$. The Rankine–Hugoniot (RH) conditions are obtained by equating the conserved fluxes F^{m} (19), F^{p} (20), and F^{e} (24) at $x = \pm\infty$,

$$(\rho u)_{-\infty} = (\rho u)_\infty, \quad (\rho u^2 + p)_{-\infty} = (\rho u^2 + p)_\infty,$$

and

$$\left(\frac{1}{2}\rho u^2 u + \frac{\gamma}{\gamma - 1}pu\right)_{-\infty} = \left(\frac{1}{2}\rho u^2 u + \frac{\gamma}{\gamma - 1}pu\right)_\infty. \tag{66}$$

In our $\gamma = 2$ cavitons (53), the flow is subsonic at $x = \pm\infty$ and supersonic at $x = 0$. We exploit this in trying to find a shock-like steady solution by patching half a caviton with a constant solution. Thus, we seek a steady solution where $\rho(x) \equiv \rho_\infty$ in the pre-shock medium and is the left half of a caviton for $x < 0$. The half-caviton profile is got from (53) by taking the reference location $x_\circ = -\infty$ so that $\rho_\circ = \rho_{-\infty}$ and $\kappa_\circ = 0$,

$$\rho(x) = \rho_{-\infty}\left[1 - (1 - M_{-\infty}^2)\,\mathrm{sech}^2\left[\sqrt{\frac{1 - M_{-\infty}^2}{4}}\,\frac{x}{\lambda_{-\infty}}\right]\right]$$

for

$$x < 0 \quad \text{with} \quad 0 \le M_{-\infty}^2 \le 1. \tag{67}$$

Here, $\lambda_{-\infty}^2 = \beta_*/c_{-\infty}^2$. On the other hand, $\rho_{+\infty}$ must correspond to a constant solution with fluxes $F_\infty^{\mathrm{m,\,p,\,e}}$. It can take one of the two density values corresponding to the X/O point (A2),

$$\rho_\infty^{\mathrm{X,O}} = \frac{F_\infty^{\mathrm{m}}\left(2F_\infty^{\mathrm{p}} \pm \sqrt{\Delta_\infty}\right)}{2F_\infty^{\mathrm{e}}} \quad \text{with} \quad \Delta = 4\left(F_\infty^{\mathrm{p}}\right)^2 - 6F_\infty^{\mathrm{e}}F_\infty^{\mathrm{m}}. \tag{68}$$

We now attempt to patch these two solutions, requiring ρ and ρ_x to be continuous at $x = 0$. Since ρ has a local minimum at the trough of a caviton, $\rho_x(0^-) = 0 = \rho_x(0^+)$ of the undisturbed medium. However, a difficulty arises in trying to ensure that ρ is continuous

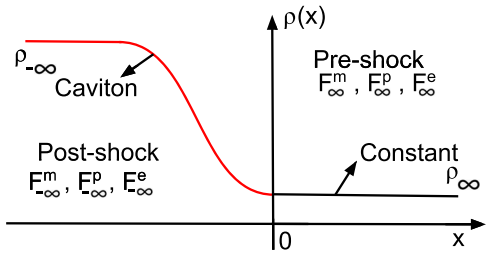

FIG. 4. Steady shock-like profiles from patching half a caviton with a constant state violate one or more Rankine–Hugoniot conditions.

at $x = 0$. Indeed, suppose we impose the RH conditions $F^{\rm m}_{\infty} = F^{\rm m}_{-\infty}$, $F^{\rm p}_{-\infty} = F^{\rm p}_{\infty}$, and $F^{\rm e}_{-\infty} = F^{\rm e}_{\infty}$, then both the pre- and post-shock regions correspond to a common phase portrait. We observe [see also Fig. 9(a)] that the caviton trough density $\rho(0^-) = \rho_{-\infty} M^2_{-\infty}$ is strictly less than both $\rho^{\rm X,O}_{\infty}$. Thus, the post-shock semi-caviton solution cannot be continuously extended into the pre-shock region.

Stated differently, in the above patched shock construction, if $\rho_{+\infty}$ is chosen to be equal to $\rho(0^-)$ in order to make ρ continuous, then the RH conditions are violated. Let us illustrate this with a $\gamma = 2$ aerostatic example. We take the pre-shock region to be vacuum ($\rho = u = p \equiv 0$ for $x > 0$) and try to patch this at $x = 0$ with the left half of the aerostatic caviton [$\rho(x) = \rho_{-\infty} \tanh^2(x/2\lambda_{-\infty})$ and $u \equiv 0$] of (55). This caviton corresponds to the values $F^{\rm m}_{-\infty} = F^{\rm e}_{-\infty} = \kappa_{-\infty} = M_{-\infty} = 0$ and has trough density $\rho(0^-) = 0$ with trough density gradient $\rho_x(0^-) = 0$ as well. Since the caviton is isentropic, its trough pressure $p(0^-) = K\rho(0^-)^2 = 0$. Thus, ρ and p are both C^1 at $x = 0$, while $u \equiv 0$ so that this is a weak solution in the sense of Sec. V A. However, it violates the RH conditions: while $F^{\rm m} \equiv 0$ is continuous, $F^{\rm p}$ and $F^{\rm u}$ are not. In fact, in the pre-shock vacuum region, $F^{\rm p} = F^{\rm u} = 0$, while in the post-shock region, they are non-zero, as evaluating them at $x = -\infty$ shows

$$F^{\rm p}_{-\infty} = p(-\infty) = K_- \rho^2_{-\infty} \neq 0 \quad \text{and} \quad F^{\rm u}_{-\infty} = 2K_- \rho_{-\infty} \neq 0. \tag{69}$$

In the post-shock region, $K_- = F^{\rm p}_{-\infty}/\rho^2_{-\infty} \neq 0$, whereas in the pre-shock vacuum, K is arbitrary since $p = \rho = 0$ for $x > 0$. In conclusion, there are no continuous steady shock-like solutions in the shock frame that satisfy the RH conditions. To see how initial conditions (ICs) that would lead to shocks in the ideal model are regularized, we turn to a numerical approach.

VI. NUMERICAL SOLUTIONS TO THE INITIAL VALUE PROBLEM

A. Spectral method with nonlinear terms isolated

In this section, we discuss the numerical solution of the isentropic R-gas dynamic initial value problem (IVP). It is convenient to work with the nondimensional variables $\hat\rho$, $\hat u$, and $\hat s$ of Sec. IV A. The continuity equation is $\hat\rho_{\hat t} + (\hat\rho\hat u)_{\hat x} = 0$, while for isentropic flow, $\hat s$ is a global constant, which may be taken to vanish by adding a constant to entropy. Thus, we can eliminate $\hat p = \hat\rho^\gamma$ in the velocity and momentum equations, both of which are in conservation form (30),

$$\hat u_{\hat t} + \left[\frac{1}{2}\hat u^2 + \frac{1}{\gamma-1}\hat\rho^{\gamma-1} - \varepsilon^2\left(\frac{\hat\rho_{\hat x\hat x}}{\hat\rho} - \frac{1}{2}\frac{\hat\rho^2_{\hat x}}{\hat\rho^2}\right)\right]_{\hat x} = 0$$

or

$$(\hat\rho\hat u)_{\hat t} + \left[\hat\rho\hat u^2 + \frac{1}{\gamma}\hat\rho^\gamma - \varepsilon^2\left(\hat\rho_{\hat x\hat x} - \frac{\hat\rho^2_{\hat x}}{\hat\rho}\right)\right]_{\hat x} = 0. \tag{70}$$

The energy equation is $\partial_{\hat t}\hat{\mathscr{E}} + \hat F^{\rm e}_{\hat x} = 0$, where the energy density and flux are

$$\hat{\mathscr{E}} = \frac{1}{2}\hat\rho\hat u^2 + \frac{\hat\rho^\gamma}{\gamma(\gamma-1)} + \frac{\varepsilon^2}{2}\frac{\hat\rho^2_{\hat x}}{\hat\rho}$$

and

$$\hat F^{\rm e} = \left[\frac{\hat\rho\hat u^2}{2} + \frac{\hat\rho^\gamma}{\gamma-1}\right]\hat u - \varepsilon^2\left[\hat u\hat\rho_{\hat x\hat x} - \frac{3}{2}\frac{\hat u\hat\rho^2_{\hat x}}{\hat\rho} - \hat u_{\hat x}\hat\rho_{\hat x}\right]. \tag{71}$$

These equations follow from the PB $\{\hat\rho(\hat x), \hat u(\hat y)\} = \partial_{\hat y}\delta(\hat x - \hat y)$ and the Hamiltonian

$$\hat H = \int\left[\frac{1}{2}\hat\rho\hat u^2 + \frac{\hat\rho^\gamma}{\gamma(\gamma-1)} + \frac{\varepsilon^2}{2}\frac{\hat\rho^2_{\hat x}}{\hat\rho}\right]d\hat x. \tag{72}$$

We will consider ICs that are fluctuations around a uniform state. For stability of the numerics, we separate the linear and nonlinear terms in the equations and treat the former implicitly and the latter explicitly. Introducing the book-keeping parameter δ (which will also enter through the ICs and may eventually be set to 1), we write

$$\hat\rho(\hat x,\hat t) = 1 + \delta\,\tilde\rho(\hat x,\hat t) \quad \text{and} \quad \hat u(\hat x,\hat t) = \bar u(\hat x,\hat t) + \delta\,\tilde u(\hat x,\hat t). \tag{73}$$

We will consider flow in the domain $-\pi \le \hat x \le \pi$ with periodic BCs and thus expand $\tilde\rho$ and $\tilde u$ as

$$\tilde\rho = \sum_{-\infty}^{\infty}\rho_n(\hat t)e^{in\hat x}, \quad \tilde u = \sum_{-\infty}^{\infty}u_n(\hat t)e^{in\hat x} \ \text{ with } \ (\rho,u)_{-n} = (\rho,u)^*_n. \tag{74}$$

Since $\int\hat\rho\,d\hat x$ is conserved, ρ_0 can be taken time-independent. Furthermore, we choose the constant $\bar\rho$ used to nondimensionalize ρ as the (conserved) average density so that $\rho_0 = 0$. We also suppose that the "background' flow velocity $\bar u$ is independent of position $\hat x$. Since $\int\hat u\,d\hat x$ is conserved and $\int\hat u\,d\hat x = 2\pi(\bar u(\hat t) + \delta\,u_0(\hat t))$, we may absorb $\delta\,u_0(\hat t)$ into $\bar u(\hat t)$ and thereby take $u_0 = 0$. Next, we write the continuity equation with nonlinear terms isolated,

$$\tilde\rho_{\hat t} = -(\bar u\tilde\rho + \tilde u)_{\hat x} - \delta\,\mathscr{F}^{\rm m}, \quad \text{where} \quad \mathscr{F}^{\rm m} = (\tilde\rho\tilde u)_{\hat x}. \tag{75}$$

The velocity equation (70) in conservation form is

$$\delta\tilde u_{\hat t} + \left(\frac{(\bar u+\delta\tilde u)^2}{2} + \frac{1}{\gamma-1}(1+\delta\tilde\rho)^{\gamma-1}\right)_x - \varepsilon^2\delta\left(\frac{\tilde\rho_{\hat x\hat x}}{1+\delta\tilde\rho} - \frac{\delta}{2}\frac{\tilde\rho^2_{\hat x}}{(1+\delta\tilde\rho)^2}\right)_{\hat x} = 0. \tag{76}$$

Separating out the linear part, we get

$$\tilde u_{\hat t} = -\left(\bar u\tilde u + \tilde\rho - \varepsilon^2\tilde\rho_{\hat x\hat x}\right)_{\hat x} - \delta\mathscr{F}^{\rm u},$$

where

$$\mathscr{F}^{\rm u} = \left(\frac{\tilde u^2}{2} + \frac{1}{\delta^2}\frac{1}{\gamma-1}\left\{(1+\delta\tilde\rho)^{\gamma-1} - \delta(\gamma-1)\tilde\rho\right\}\right)_x + \left(\frac{\varepsilon^2}{(1+\delta\tilde\rho)^2}\left(\tilde\rho\tilde\rho_{\hat x\hat x}(1+\delta\tilde\rho) + \frac{1}{2}\tilde\rho^2_{\hat x}\right)\right)_{\hat x}. \tag{77}$$

In (75) and (77), the linear terms are at $\mathscr{O}(\delta^0)$, while the nonlinearities involve δ to higher powers, depending on the value of γ. Interestingly, for $\gamma = 2$, the pressure gradient does not contribute to the nonlinear part of the acceleration,

$$\mathscr{F}^{\rm u}_{\gamma=2} = \left[\frac{\tilde u^2}{2} + \frac{\varepsilon^2}{(1+\delta\tilde\rho)^2}\left(\tilde\rho\tilde\rho_{\hat x\hat x}(1+\delta\tilde\rho) + \frac{1}{2}\tilde\rho^2_{\hat x}\right)\right]_{\hat x}. \tag{78}$$

Expanding $\mathscr{F}^{\rm m} = \sum_n\mathscr{F}^{\rm m}_n e^{in\hat x}$ and $\mathscr{F}^{\rm u} = \sum_n\mathscr{F}^{\rm u}_n e^{in\hat x}$, the EOM in Fourier space become

$$\dot\rho_n = -in(\bar u\rho_n + u_n) - \delta\mathscr{F}^{\rm m}_n$$

and

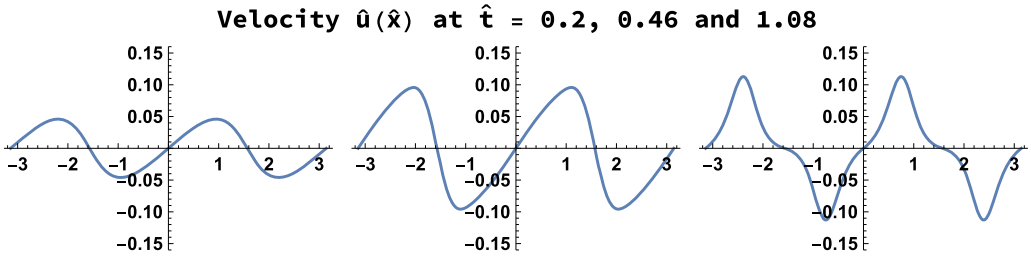

FIG. 5. Evolution of velocity for IC $\hat{\rho} = 1 + 0.1\cos 2\hat{x}$ and $\hat{u} = 0$, showing how the gradient catastrophe is averted through the formation of a pair of solitary waves in the velocity profile.

$$\dot{u}_n = -in(\tilde{u}u_n + (1+\varepsilon^2 n^2)\rho_n) - \delta\mathscr{F}_n^{\mathrm{u}}. \tag{79}$$

When nonlinearities ($\mathscr{F}^{\mathrm{m}}$, $\mathscr{F}^{\mathrm{u}}$) are ignored and we assume $(\rho_n(t), u_n(t) \propto e^{-i\omega_n t})$, one finds the dispersion relation $(\omega_n - n\tilde{u})^2 = n^2(1+\varepsilon^2 n^2)$ familiar from Sec. IV A. To deal with the fully nonlinear evolution given by (79), we use a semi-implicit numerical scheme outlined in Appendix D.

B. Numerical results: Avoidance of gradient catastrophe, solitons, and recurrence

The above numerical scheme for $\gamma = 2$ is implemented by truncating the Fourier series after $n_{\max} = 16$ modes. The evolution is done for 750 time steps $(0 \le \hat{t} \le 15)$, each of size $\Delta = 0.02$, starting with the nondimensional ICs,

$$\hat{\rho}(\hat{x},0) = 1 + \delta\tilde{\rho}(\hat{x},0) \quad \text{and} \quad \hat{u}(\hat{x},0) = 0,$$

where

$$\tilde{\rho}(\hat{x},0) = \sin\hat{x} \quad \text{or} \quad \cos 2\hat{x} \quad \text{and} \quad \delta = 0.1. \tag{80}$$

We find that at early times, where $\hat{u}$ has a negative slope, its gradient increases and decreases where the slope is positive. Without the regularization ($\varepsilon = 0$), the higher Fourier modes can then get activated and the velocity and density profiles become highly oscillatory with steep gradients. Moreover, amplitudes begin to grow and the code eventually ceases to conserve energy and momentum.

By contrast, in the presence of the regularization (say, $\varepsilon = 0.2$), we find that the above gradient catastrophe is averted and energy is conserved (to about 3 parts in 1000), while momentum is conserved to machine precision. In fact, we find that the real and imaginary parts Q_r and Q_i of the next conserved quantity (96) are also conserved. Interestingly, when u develops a steep negative gradient, a pair of solitary waves emerge at the top (wave of elevation) and bottom (wave of depression) of the u profile and the gradient catastrophe is avoided (see Fig. 5). This mechanism by which the incipient shock-like discontinuity is regularized is to be contrasted with KdV, where an entire train of solitary waves can form.[34] However, as with KdV, our solitary waves can suffer a head-on collision and pass through each other. After the collision, they re-emerge with roughly similar shapes and a phase shift. Figure 6 shows the space-time trajectories of the centers of several of these solitary waves, showing their collisions.

We also find that higher modes u_n and ρ_n ($n \gtrsim 9$) grow from zero, but soon saturate and remain a few orders of magnitude below the first few modes (see Fig. 7). This justifies truncating the Fourier series at $n_{\max} = 16$. The modes also display an approximate periodicity in time. This suggests recurrent motion.[35–37] This behavior is also captured in Fig. 8(a) where we plot the Rayleigh quotient or the mean square mode number

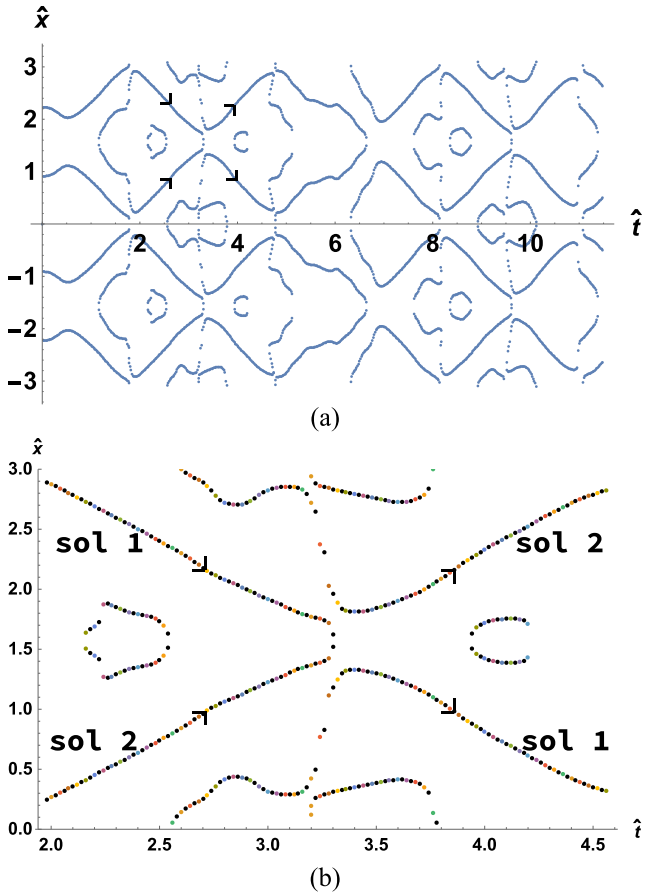

FIG. 6. (a) Space-time trajectories of the "centers" of "solitary waves" in the velocity profile (for the initial condition $\hat{\rho} = 1 + 0.1\cos 2\hat{x}$ and $\hat{u} = 0$) showing several collisions. The locations of the "centers" are determined by finding the maxima/minima of $\hat{u}$ at each instant of time. (b) Close-up of one collision of solitary waves (sol 1 and sol 2), showing approximate asymptotic straight-line trajectories and phase shifts. The figures include the trajectories of the crests/troughs of small ripples that typically arise and go away in pairs, but do not qualify as solitary waves.

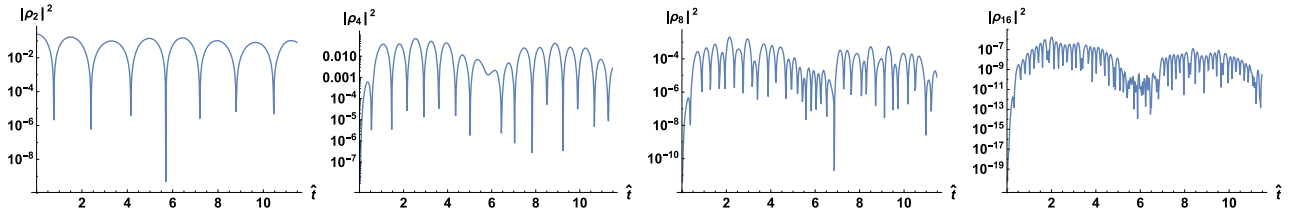

FIG. 7. Time evolution of Fourier modes $|\rho_n|^2$ for $n = 2$, 4, 8, and 16 for IC $\tilde{\rho} = \cos 2\hat{x}$ and $\tilde{u} = 0$ showing that the higher modes remain uniformly small compared to the first few, justifying truncation of Fourier series.

$$R = \frac{\int |\hat{\rho}_{\hat{x}}|^2 d\hat{x}}{\int |\hat{\rho}|^2 d\hat{x}} = \frac{\sum_n n^2 |\rho_n|^2}{\sum_n |\rho_n|^2} \tag{81}$$

as a function of time. It is found to fluctuate between bounded limits indicating that effectively only a finite number of modes participate in the dynamics. Another interesting statistic is the spectral distribution of energy (E_n) and its dependence on time. Figure 8(b) shows the time evolution of log E_n for $n = 2$, 6, 10, and 16 for the IC $\tilde{\rho} = \cos 2\hat{x}$ and $\tilde{u} = 0$ and demonstrates that the energy in the higher modes remains small. Moreover, each mode ρ_n and u_n oscillates between an upper and lower bound and shows approximate periodicity with differing periods. In Fig. 8(c), log E_n vs n is plotted for a few values of $\hat{t}$. Unlike the power law decay $n^{-5/3}$ in the inertial range of fully developed turbulence, here we see that E_n drops exponentially with n. In particular, there is no equipartition of energy among the modes.

VII. CONNECTION TO NONLINEAR SCHRÖDINGER AND GENERALIZATIONS

Our numerical results indicate recurrence and soliton-like scattering in 1D isentropic R-gas dynamics for $\gamma = 2$, suggesting integrability. Remarkably, in this case, R-gas dynamics is transformable into the defocusing (repulsive) cubic nonlinear Schrödinger equation (NLSE). More generally, adiabatic R-gas dynamics may be viewed as a novel generalization of the NLSE. Indeed, let us write the velocity field as $\mathbf{v} = \nabla\phi + \frac{\lambda\nabla\mu}{\rho} + \frac{\alpha\nabla s}{\rho}$, where s is the specific entropy and α, λ, and μ are Clebsch potentials.[27] As in treatments of superfluidity[19,38] and "quantum hydrodynamics,"[20] if we define the Madelung transform, $\psi(\mathbf{r}, t) = \sqrt{\rho}\exp(i\phi(\mathbf{r})/2\sqrt{\beta_*})$, then the R-gas dynamic energy density (4) becomes

$$\mathscr{E} = 2\beta_*|\nabla\psi|^2 + 2\frac{\sqrt{\beta_*}}{|\psi|^2}(\alpha\nabla s + \lambda\nabla\mu)\cdot\left(\frac{\psi^*\nabla\psi - \psi\nabla\psi^*}{2i}\right) + \frac{\lambda\alpha}{|\psi|^2}\nabla\mu\cdot\nabla s + \frac{\alpha^2(\nabla s)^2 + \lambda^2(\nabla\mu)^2}{2|\psi|^2} + \frac{\tilde{p}e^{s/c_V}}{(\gamma-1)}\frac{|\psi|^{2\gamma}}{\tilde{\rho}^\gamma}. \tag{82}$$

Here, $\tilde{p}$ and $\tilde{\rho}$ are constant reference pressure and density, respectively. The transformation from (ρ, ϕ) to $(\psi, \psi*)$ is canonical. The corresponding equations of motion for ψ, α, λ, μ, and s may be obtained using the canonical bosonic PBs $\{\psi(\mathbf{r}), \psi^*(\mathbf{r}')\} = -(i/2\sqrt{\beta_*})\delta(\mathbf{r} - \mathbf{r}')$, $\{\lambda(\mathbf{r}), \mu(\mathbf{r}')\} = \delta(\mathbf{r} - \mathbf{r}')$, and $\{\alpha(\mathbf{r}), s(\mathbf{r}')\} = \delta(\mathbf{r} - \mathbf{r}')$.

Specializing to isentropic potential flow where $s = \bar{s}$ is constant, $p = K(\gamma - 1)\rho^\gamma$ (29), and $\mathbf{v} = \nabla\phi$, (82) simplifies to

$$H = \int \left[2\beta_*|\nabla\psi|^2 + K|\psi|^{2\gamma}\right]d\mathbf{r}. \tag{83}$$

Using the above PBs for ψ, one finds that ψ satisfies the *defocusing* nonlinear Schrödinger equation

$$i\sqrt{\beta_*}\psi_t = -\beta_*\nabla^2\psi + \frac{1}{2}\gamma K|\psi|^{2(\gamma-1)}\psi. \tag{84}$$

Interestingly, in one dimension, the R-gas dynamic form of the *focusing* cubic ($\gamma = 2$) NLSE had been obtained in the context of the Heisenberg magnetic chain.[39,40] However, as noted in Ref. 39, the Heisenberg chain leads to negative pressure! Returning to (84), we see that the real and imaginary parts of the NLSE correspond to the

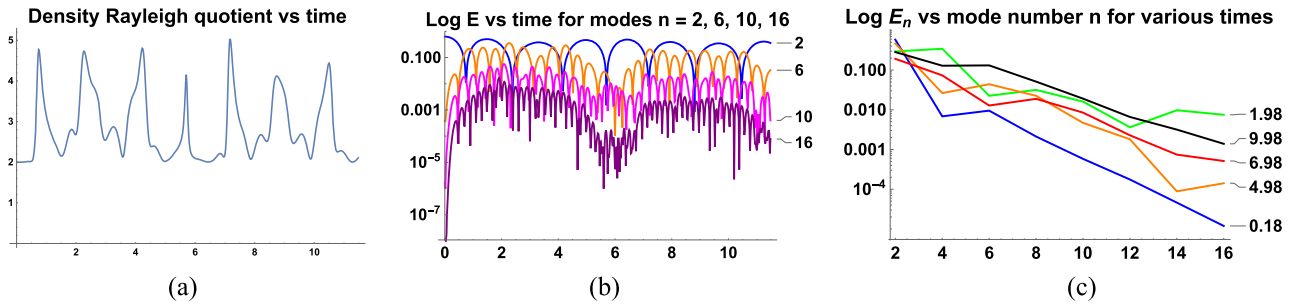

FIG. 8. (a) Rayleigh quotient displays bounded oscillations indicating only a few modes are active. (b) Time evolution of log E_n for modes $n = 2$, 6, 10, and 16. The higher modes remain small with each one showing approximately periodic oscillations. (c) log E_n vs n for a few values of $\hat{t}$ showing exponential drop with n. In all cases, the IC was $\tilde{\rho} = \cos 2\hat{x}$ and $\tilde{u} = 0$.

Bernoulli and continuity equations. The $\nabla^2\psi$ term leads to the divergence of the mass flux, $\mathbf{v}^2$, and regularization terms in the isentropic R-gas dynamic equations

$$\rho_t + \nabla\cdot(\rho\mathbf{v}) = 0 \quad \text{and} \quad \phi_t = -\gamma K\rho^{\gamma-1} - \frac{\mathbf{v}^2}{2} + 2\beta_*\frac{\nabla^2\sqrt{\rho}}{\sqrt{\rho}}. \tag{85}$$

Evidently, β_* plays the role of $\hbar^2$. The nonlinear term $(\gamma K/2)|\psi|^{2(\gamma-1)}\psi$ corresponds to the isentropic pressure $p = (\gamma-1)K\rho^\gamma$ whose positivity implies that we get the defocusing/repulsive NLSE. Thus, our regularization term $2\beta_*(\nabla^2\sqrt{\rho})/\sqrt{\rho}$ is like a quantum correction to the classical isentropic pressure. For $\gamma = 2$, we get the cubic NLSE or Gross–Pitaevskii equation (without an external trapping potential). Note that 1D isentropic flow on the line with $\mathbf{v} = (u(x), 0, 0)$ is always potential flow: $u = \phi_x$. So the above transformation takes 1D isentropic R-gas dynamics (30) to the defocusing 1D NLSE, which for $\gamma = 2$ and periodic BCs admits infinitely many conserved quantities in involution.[24] This explains our numerical observations of approximate phase shift scattering of solitary waves and recurrence.

A. NLSE interpretation of steady R-gas dynamic cavitons and cnoidal waves

It turns out that the steady solutions of 1D isentropic R-gas dynamics (Sec. IV B) correspond to NLSE wavefunctions ψ with harmonic time dependence. For $\gamma = 2$, our aerostatic caviton corresponds to the dark soliton of NLSE. More generally, aerostatic steady solutions correspond to ψ of the form $\sqrt{\rho(x)}\exp(-iF^{\mathrm{u}}t/2\sqrt{\beta_*})$, where F^{u} is the constant velocity flux (31). Finally, non-aerostatic cnoidal waves correspond to interesting asymptotically plane wave NLSE wavefunctions modulated by a periodic cnoidal amplitude. Here, we consider the cavitons and cn waves in increasing order of complexity.

Aerostatic caviton: The simplest caviton solution of Sec. IV B 3 is aerostatic,

$$\rho(x) = \rho_\circ\tanh^2\left(\frac{x}{2\lambda_\circ}\right), \quad u(x) = 0,$$

and

$$p(x) = K\rho^2, \quad \text{where} \quad K = \frac{c_\circ^2}{2\rho_\circ}. \tag{86}$$

Here, $\rho_\circ$, $\lambda_\circ$, and $c_\circ^2$ are positive constants. The corresponding specific enthalpy and velocity flux are

$$h = 2\,K\rho = c_\circ^2\tanh^2\left(\frac{x}{2\lambda_\circ}\right)$$

and

$$F^{\mathrm{u}} = \frac{u^2}{2} + h - 2\beta_*\frac{(\sqrt{\rho})_{xx}}{\sqrt{\rho}} = c_\circ^2, \quad \text{where} \quad \beta_* = \lambda_\circ^2 c_\circ^2. \tag{87}$$

Thus, the Bernoulli equation $\phi_t + F^{\mathrm{u}} = 0$ (31) is satisfied, provided we take the velocity potential $\phi = -c_\circ^2\,t$ to be time-dependent. The resulting ψ is the dark soliton solution of the defocusing NLSE (see Sec. 6.6 of Ref. 2)

$$\psi = \sqrt{\rho}\,\exp\left(\frac{i\phi}{2\sqrt{\beta_*}}\right) = \sqrt{\rho_\circ}\tanh\left(\frac{x}{2\lambda_\circ}\right)e^{-\frac{ic_\circ^2 t}{2\sqrt{\beta_*}}}. \tag{88}$$

Non-aerostatic caviton: More generally, for a non-aerostatic caviton (for $0 < M_\circ < 1$ and $\rho_\circ$, $\lambda_\circ$ and $c_\circ^2$ positive constants),

$$\rho(x) = \rho_\circ\left(1 - (1-M_\circ^2)\,\mathrm{sech}^2\left(\sqrt{\frac{1-M_\circ^2}{4}}\frac{x}{\lambda_\circ}\right)\right),$$
$$u(x) = \frac{c_\circ M_\circ\rho_\circ}{\rho(x)}, \quad \text{and} \quad p(x) = \frac{c_\circ^2}{2\rho_\circ}\rho(x)^2. \tag{89}$$

In this case, the constant velocity flux is $F^{\mathrm{u}} = c_\circ^2(2+M_\circ^2)/2$. The resulting velocity potential is

$$\phi = -\frac{1}{2}c_\circ^2(2+M_\circ^2)t + c_\circ M_\circ x + 2c_\circ\lambda_\circ\arctan\left(\frac{\sqrt{1-M_\circ^2}}{M_\circ}\tanh\left(\frac{\sqrt{1-M_\circ^2}}{2\lambda_\circ}x\right)\right). \tag{90}$$

Thus, ψ is asymptotically a plane wave with phase speed $c_\circ(2+M_\circ^2)/2M_\circ$. This ψ may be regarded as a high-frequency carrier wave modulated by a localized signal.

Aerostatic snoidal waves: The simplest steady periodic solutions is the aerostatic snoidal wave (54),

$$u \equiv 0, \quad \rho = \rho_\circ(1-2\kappa_\circ)\,\mathrm{sn}^2\left(\frac{x}{2\lambda_\circ}, 1-2\kappa_\circ\right) \text{ for } 0 < \kappa_\circ < \frac{1}{2}. \tag{91}$$

Here, $F^{\mathrm{u}} = c_\circ^2(1-\kappa_\circ)$ and $\phi = -F^{\mathrm{u}}t$. The resulting ψ is a snoidal wave with harmonic time dependence,

$$\psi = \sqrt{\rho_\circ(1-2\kappa_\circ)}\,\mathrm{sn}\left(\frac{x}{2\lambda_\circ}, 1-2\kappa_\circ\right)e^{-\frac{ic_\circ^2(1-\kappa_\circ)\,t}{2\sqrt{\beta_*}}}. \tag{92}$$

Non-aerostatic cnoidal waves: Finally, in the general case, we have from (51),

$$\rho(x) = \rho_\circ\left[\tilde\rho_+ - (\tilde\rho_+ - \tilde\rho_-)\,\mathrm{cn}^2\left(\frac{\sqrt{1-\tilde\rho_-}}{2}\frac{x}{\lambda_\circ}, \frac{\tilde\rho_+ - \tilde\rho_-}{1-\tilde\rho_-}\right)\right],$$
$$u(x) = \frac{c_\circ M_\circ\rho_\circ}{\rho(x)}, \quad \text{and} \quad p(x) = \frac{c_\circ^2}{2\rho_\circ}\rho(x)^2, \tag{93}$$

where $0 < \kappa_\circ < 1/2$ and $0 < M_\circ < 1 - \sqrt{2\kappa_\circ}$ [lower triangular region of Fig. 3(a)]. Here, $\tilde\rho_\pm(\kappa_\circ, M_\circ)$ are as in (48). Furthermore, $\rho_\circ$, $c_\circ^2$, and $\lambda_\circ$ are positive constants that set scales. As before, $\phi = -F^{\mathrm{u}}t + \int_0^x u(x')\,dx'$, where the constant velocity flux F^{u} depends on $c_\circ$, $\kappa_\circ$, and $M_\circ$, but is independent of $\rho_\circ$ and $\lambda_\circ$. Although an explicit formula for $\phi(x, t)$ is not easily obtainable, it is evident that for large x, ϕ grows linearly in x with a subleading oscillatory contribution. Thus, ψ has a purely harmonic time-dependence $\exp\left(-iF^{\mathrm{u}}t/2\sqrt{\beta_*}\right)$, a periodic cnoidal modulus $|\psi| = \sqrt{\rho(x)}$, and an argument that asymptotically grows linearly in x. Thus, asymptotically, ψ is a plane wave modulated by the periodic amplitude $\sqrt{\rho(x)}$.

B. Conserved quantities and Rayleigh quotient of NLSE and R-gas dynamics

The cubic 1D NLSE admits an infinite tower of conserved quantities. The first three are

$$N = \int |\psi|^2\, dx, \quad P_{\rm NLSE} = \int \Im(\psi^* \psi_x)\, dx,$$

and

$$E_{\rm NLSE} = \int \left(|\psi_x|^2 + \frac{K}{2\beta_*} |\psi|^4 \right) \beta_*^{1/4} dx. \tag{94}$$

These correspond to the mass $M = N$, momentum $P = 2\sqrt{\beta_*} P_{\rm NLSE}$, and energy $H = 2\beta_*^{3/4} E_{\rm NLSE}$ of R-gas dynamics. The next conserved quantity of NLSE (with periodic BCs) is[24]

$$Q = \int_{-L}^{L} \left[\sqrt{\beta_*}\, \psi^* \psi_{xxx} - \frac{K|\psi|^2}{2\sqrt{\beta_*}} (\psi \psi_x^* + 4\psi^* \psi_x) \right] dx. \tag{95}$$

$\Re Q$ and $\Im Q$ correspond to the following in R-gas dynamics:

$$Q_r = \frac{3\sqrt{\beta_*}}{4} \int_{-L}^{L} \left(\frac{\rho_x^3}{2\rho^2} - \frac{\rho_x \rho_{xx}}{\rho} \right) dx$$

and

$$Q_i = -\int_{-L}^{L} \left[\frac{u_x \rho_x}{2} + \frac{3u\rho_x^2}{8\rho} + \frac{u^3 \rho}{8\beta_*} + \frac{3\, Ku\rho^2}{4\beta_*} \right] dx. \tag{96}$$

In Sec. VI A, we use the conservation of Q_r and Q_i to test our numerical scheme. In Ref. 35, it was shown that for the cubic 1D NLSE, the Rayleigh quotient or mean square mode number for periodic BCs,

$$R_{\rm NLSE} = \frac{\int_{-L}^{L} |\psi_x|^2\, dx}{\int_{-l}^{l} |\psi|^2\, dx}, \tag{97}$$

is related to the number of active degrees of freedom and is bounded in both focusing and defocusing cases. This has a simple interpretation in R-gas dynamics, since

$$R_{\rm NLSE} = \frac{1}{2\beta_* M} \int_{-L}^{L} \left(\frac{1}{2} \rho u^2 + \frac{\beta_*}{2} \frac{\rho_x^2}{\rho} \right) dx \le \frac{H}{2\beta_* M}. \tag{98}$$

Consequently, 1D isentropic R-gas dynamic potential flows are recurrent in the sense discussed in Ref. 35.

VIII. DISCUSSION

It is a significant feature of our attempt to conservatively regularize singularities in gas dynamics that it has led us (in the case of isentropic potential flow) to the *defocusing* NLSE. Heuristically, the defocusing interaction tends to amplify linear dispersive effects and thereby prevent blowups. For $\gamma = 2$, this connection to the cubic NLSE should provide powerful tools [including the inverse scattering transform in one dimension (see Refs. 24 and 41 and Sec. 9.10 of Ref. 2)] to deal with the initial-boundary value problems in various dimensions as well as alternative numerical schemes. Moreover, the bound on the NLSE Rayleigh quotient obtained in Ref. 35 (see also Sec. VII B) generalizes to two and three dimensions as well as to nonlinearities other than cubic ($\gamma \neq 2$). This would have implications for recurrence in more general R-gas dynamic isentropic potential flows even in the absence of integrability. The techniques of dispersive shock wave theory[1,4,42] could provide additional tools to address R-gas dynamic flows.

In Refs. 43 and 44, a classification of semilinear PDEs [perturbations of linear equations by lower order nonlinear terms] into subcritical, critical, and supercritical based on conserved quantities (mass and energy), scaling symmetries, and regularity of the initial data is described. Although the equations of R-gas dynamics given in Sec. II are not semilinear, in the special case of isentropic potential flow, the transformation to NLSE makes them semilinear. It is thus interesting to examine the implications of this classification for R-gas dynamics. For example, the critical scaling regularity[43] of NLSE in d spatial dimensions is $s_c = d/2 - 1/(\gamma - 1)$. Thus, if the initial data are such that the number of particles and energy are finite (so that ψ, $\nabla\psi \in L^2$ and $\psi \in H^1$), then according to the scaling heuristic, the NLSE is subcritical for any $\gamma > 1$ in one and two dimensions and also for $1 < \gamma < 3$ in three dimensions.

In Sec. V B, we argued that 1D R-gas dynamics does not admit any continuous shock-like steady solutions. In fact, we found that if we try to patch half a caviton at its trough density with a constant state, then the Rankine–Hugoniot conditions are violated. We conjecture that this absence of steady shock-like solutions is a general feature of a wide class of conservatively regularized gas dynamic models. Loosely, this is like d'Alembert's "theorem" that continuous solutions of Euler's equations cannot ever lead to drag, although possibly to lift. On the other hand, inclusion of viscosity *does* permit drag as well as steady shock-like solutions as in Burgers.[1,2] Allowing for non-steady solutions, we find that in R-gas dynamics, the gradient catastrophe is averted through the formation of a pair of solitary waves (see Sec. VI B). It would be interesting to see if this mechanism is observed in any physical system, say, one where dissipative effects are small as in nonlinear optics, weak shocks, cold atomic gases, or superfluids. For further discussion on steepening gradients and criteria for detecting wave breaking in dispersive hydrodynamics, see Refs. 45 and 46.

Intriguingly, the negative pressure ($p = -\rho^2/8$[39]), $\gamma = 2$ isentropic R-gas dynamic equations for $\beta_* = 1/2$ in one dimension (30) are equivalent to the vortex filament equation $\dot{\xi} = G\xi' \times \xi''$ for a filament ξ with curvature $\kappa = \sqrt{\rho}$ and torsion $\tau = u$[40] when $G = 1/2$. Furthermore, it is well-known[47] that the vortex filament equation is related to the continuous Heisenberg magnetic chain equation $\dot{S} = GS \times S''$ with $S = \xi'$. It is noteworthy that negative pressures (relative to atmospheric pressure) can arise in real flows, for instance, in the presence of strong currents.[48] An open question is to give a geometric or magnetic chain interpretation of the positive pressure R-gas dynamic equations as well as those for other values of γ.

Although we have formulated R-gas dynamics in 3D, our analytic and numerical solutions have been restricted to one dimension. It would be interesting to extend this work to higher dimensional problems such as oblique shocks and the Sedov–Taylor spherical blast wave problem. The mechanical and thermodynamic stability of our traveling caviton and periodic wave solutions is also of interest. One also wishes to examine whether the capillarity energy considered here arises from kinetic theory in a suitable scaling limit of small Knudsen numbers as for the Korteweg equation.[16,49] Finally, our Hamiltonian and Lagrangian formulations of R-gas dynamics can be used as starting points in formulating the quantum theory. The transformation to NLSE provides another approach to quantization for isentropic potential flow, especially when $\gamma = 2$. Although we have focused on the conservatively regularized model, a more complete and realistic treatment would have to include viscous dissipation just as in the KdV–Burgers equation.

Our attempt to generalize KdV to include the adiabatic dynamics of density, velocity, and pressure has led to an interesting link between KdV and NLSE that is quite different from the well known ones (see, e.g., Ref. 2). In fact, we may view R-gas dynamics as a natural generalization of both. While it extends the KdV idea of a minimal conservative dispersive regularization to adiabatic gas dynamics in any dimension and shares with it the cnoidal and sech^2 solutions, it also reduces to the defocusing cubic NLSE for isentropic potential flow of a gas with adiabatic index two. Thus, the cubic 1D NLSE is a very special member of a larger class of R-gas dynamic equations that make sense in any dimension and for nonlinearities other than cubic while also allowing for adiabatically evolving entropy and vorticity distributions.

ACKNOWLEDGMENTS

A.T. gratefully acknowledges the support and hospitality of CMI. We thank the anonymous referees for suggesting references and improvements. This work was supported in part by the Infosys Foundation, J N Tata Trust, and the Science and Engineering Research Board, Government of India, via Grant Nos. CRG/2018/002040 and MTR/2018/000734.

APPENDIX A: VECTOR FIELD AND PHASE PORTRAIT FOR STEADY SOLUTIONS

With x and ρ viewed as time and position, steady, isentropic density profiles must satisfy the Newtonian ODE (39). Ignoring the velocity-dependent force, two cases arise: (a) for $F^{\mathrm{u}} < 0$, V has only bound states corresponding to periodic ρ and (b) for $F^{\mathrm{u}} > 0$, there are periodic waves and a caviton, provided V has a local minimum [this happens when F^{p} and $\Delta = (F^{\mathrm{p}})^2\gamma^2 - 2(\gamma^2-1)F^{\mathrm{u}}(F^{\mathrm{m}})^2$ are both positive]. The velocity-dependent force $\propto \rho_x^2/\rho$ is reminiscent of the drag force $\propto -|\rho_x|\rho_x$ on a body at a high Reynolds number. However, while air drag tends to decrease the speed, this force is positive and tends to increase the velocity ρ_x. Moreover, although the naive "energy" $\beta_*\rho_x^2/2 + V$ is *not* conserved, Eq. (39) is non-dissipative and, in fact, Hamiltonian (see Appendix B). Since the velocity-dependent force tends to push the particle outwards, it cannot convert a scattering state into a bound state. We also find that the qualitative nature of the phase portraits is not significantly altered by this force.

Introducing $\eta = \rho_x$, (39) defines a vector field W on the right half ρ–ρ_x phase plane,

$$\begin{pmatrix}\rho\\ \eta\end{pmatrix}_x = W \equiv \begin{pmatrix}\eta\\ -\frac{V'(\rho)}{\beta_*} + \frac{(\gamma+1)}{2}\frac{\eta^2}{\rho}\end{pmatrix}. \tag{A1}$$

Although η^2/ρ is singular along the $\rho = 0$ axis, it is "shielded" by the repulsive logarithmic potential in V. The bounded integral curves of W correspond to bounded steady densities. Fixed points (FPs) of W correspond to constant density solutions. They are located at $(\rho_{p,m}, 0)$, where $\rho_{p,m}$ are the extrema of V,

$$\rho_{p,m} = \frac{\gamma F^{\mathrm{p}} \pm \sqrt{\Delta}}{2(\gamma-1)F^{\mathrm{u}}}. \tag{A2}$$

There may be two, one, or no FPs in the physical region $\rho > 0$. We are interested in the cases where there is at least one FP in the physical region, as otherwise ρ is unbounded. This requires $\Delta > 0$. Assuming this is the case and also assuming that the flow is not aerostatic ($F^{\mathrm{m}} \neq 0$ or $u \not\equiv 0$), we find that there are two physical FPs if F^{p} and F^{u} are both positive, one fixed point if $F^{\mathrm{u}} < 0$ and none otherwise. The character of these FPs may be found by linearizing W around them. Writing $\rho = \rho_{p,m} + \delta\rho$ and $\eta = 0 + \delta\eta$, we get

$$\frac{d}{dx}\begin{pmatrix}\delta\rho\\ \delta\eta\end{pmatrix} = A\begin{pmatrix}\delta\rho\\ \delta\eta\end{pmatrix}, \quad \text{where} \quad A = \begin{pmatrix}0 & 1\\ -V''(\rho_{p,m})/\beta_* & 0\end{pmatrix}. \tag{A3}$$

The eigenvalues of the coefficient matrix A are

$$\lambda = \pm\sqrt{\frac{-V''(\rho_{p,m})}{\beta_*}}, \quad \text{where} \quad V''(\rho_{p,m}) = \mp\frac{\sqrt{\Delta}}{\rho_{p,m}}. \tag{A4}$$

Thus, the physical FPs of W must be either X or O points (saddles or centers in the linear approximation) accordingly as $V'' < 0$ (real eigenvalues) or $V'' > 0$ (imaginary eigenvalues). The Hartman–Grobman theorem guarantees that the linear saddles remain saddles even upon including nonlinearities. Moreover, the linear O-point at $(\rho_m, 0)$ is always a true O-point since we may verify that $(\rho_m, 0)$ is a minimum of the conserved quantity K (41). Thus, as summarized in Table I, there are two types of phase portraits leading to bounded solutions $\rho(x)$: (i) if F^{p} and F^{u} are both positive, then W has an O-point at $(\rho_m, 0)$ and an X-point at $(\rho_p, 0)$ to its right and (ii) if $F^{\mathrm{u}} < 0$, W has only one physical fixed point, an O-point at $(\rho_m, 0)$. As shown in Figs. 9(a) and 9(b), in case (i), we have two types of bounded solutions: periodic waves corresponding to closed curves around the O-point $(\rho_m, 0)$ and a solitary wave corresponding to the separatrix orbit that begins and ends at $(\rho_p, 0)$ and encircles the O-point. Since $\rho_p > \rho_m$, a solitary wave must be a caviton. In case (ii), the only bounded solutions $\rho(x)$ are periodic waves corresponding to the closed curves encircling the O-point $(\rho_m, 0)$, as shown in Figs. 9(c) and 9(d). Solutions with $K < 0$ have negative pressure.

TABLE I. Nature of fixed points and bounded solutions on the ρ–ρ_x half-plane. (a) General non-aerostatic case, when F^{m}, $F^{\mathrm{e}} \neq 0$ and $\Delta > 0$. (b) Aerostatic limit ($u \equiv 0$, $F^{\mathrm{m}} = F^{\mathrm{e}} = 0$). $K < 0$ corresponds to solutions with negative pressure.

F^{p}	F^{u}	Fixed point	Bounded solutions
(a) Non-aerostatic steady solutions			
+	+	O and X point	Periodic, caviton
+	−	O point	Periodic ($K < 0$)
−	−	O point	Periodic ($K < 0$)
−	+	None	None
(b) Aerostatic steady solutions			
+	+	X point	Periodic, caviton
−	−	O point	Periodic ($K < 0$)
+	−	None	Periodic ($K < 0$)
−	+	None	None
0	+	None	None
0	−	None	Elevatons ($K < 0$)
0	0	None	None

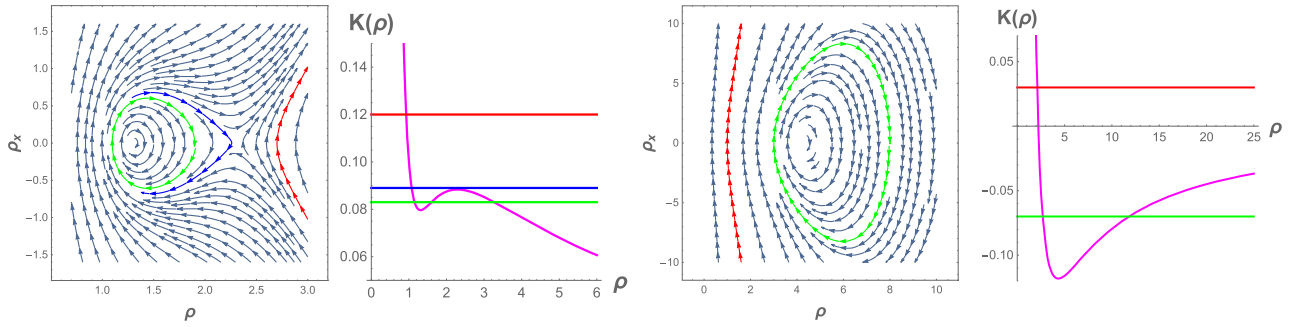

FIG. 9. [(a) and (b)] The vector field W on the ρ–ρ_x phase plane for $\gamma = 2$ and $\beta_* = 0.1$ and the entropy constant $K(\rho_\circ)$ (43) (which labels trajectories) for $F^{\rm m} = 1$, $F^{\rm p} = 0.9$, and $F^{\rm u} = 0.5$. As K is decreased from infinity, we encounter unbounded solutions followed by a bounded caviton separatrix emanating from the X-point. The caviton encircles periodic orbits around the O-point. The X and O points are the only constant solutions. [(c) and (d)] The vector field W and corresponding K for $F^{\rm m} = 1$, $F^{\rm p} = -2$, and $F^{\rm u} = -1$. Scattering states for $K > 0$ are followed by periodic orbits around the O-point with $K < 0$ and an infinite caviton separatrix at $K = 0$. Solutions with $K < 0$ have negative pressure.

Isentropic aerostatic steady solutions: In the aerostatic limit ($u \equiv 0$), both the fluxes $F^{\rm e}$ and $F^{\rm m}$ vanish, though their ratio $F^{\rm e}/F^{\rm m} = F^{\rm u}$ is finite. Equation (39) for steady solutions becomes

$$\beta_*\rho_{xx} = -V'(\rho) + \frac{(\gamma+1)\beta_*}{2}\frac{\rho_x^2}{\rho},$$

where

$$V(\rho) = \gamma F^{\rm p}\rho - (\gamma-1)\frac{F^{\rm u}}{2}\rho^2. \tag{A5}$$

In this limit, the small-ρ logarithmic barrier in V (39) is absent, and the singularity along $\rho = 0$ becomes "naked." One of the FPs in Eq. (A2) tends to (0, 0), while the other one tends to $(\gamma F^{\rm p}/(\gamma - 1)F^{\rm u}, 0)$. Table I summarizes the nature of physical fixed points and bounded solutions for various possible signs of $F^{\rm p}$ and $F^{\rm u}$. Interestingly, for $F^{\rm p} = 0$ and $F^{\rm u} < 0$, there is a family of solitary waves of *elevation*, though with negative pressure.

APPENDIX B: CANONICAL FORMALISM FOR STEADY SOLUTIONS

The equation for steady solutions (39) describes a mechanical system with 1 degree of freedom and conserved quantity $K(\rho, \rho_x)$ (41). Here, we give a canonical formulation for (39) by taking K to be the Hamiltonian. We seek a suitable PB $\{\rho, \rho_x\}$ so that Hamilton's equations $\rho_x = \{\rho, K\}$ and $\rho_{xx} = \{\rho_x, K\}$ reproduce (39). The former gives

$$\{\rho, K\} = \left\{\rho, \frac{1}{2}\frac{\beta_*\rho_x^2}{\rho^{\gamma+1}}\right\} = \rho_x$$

or

$$\frac{\beta_*\rho_x}{\rho^{\gamma+1}}\{\rho, \rho_x\} = \rho_x \quad \Rightarrow \quad \{\rho, \rho_x\} = \frac{\rho^{\gamma+1}}{\beta_*}. \tag{B1}$$

Using this PB, $\rho_{xx} = \{\rho_x, K\}$ reproduces (39). This PB is not canonical, but if we define $\varpi = \beta_*\rho_x/\rho^{\gamma+1}$, then $\{\rho, \varpi\} = 1$ so that ϖ is the momentum conjugate to ρ. The corresponding Hamiltonian is

$$K(\rho, \varpi) = \frac{1}{2}\frac{\rho^{\gamma+1}}{\beta_*}\varpi^2 + U(\rho) \tag{B2}$$

with U as in (41). The "mass" factor in the kinetic term is "position" (ρ) dependent. In terms of the contravariant "mass metric" $m^{-1}(\rho) = \rho^{\gamma+1}/\beta_*$, $K = (1/2)m^{-1}\varpi^2 + U$. The corresponding Lagrangian is

$$L = \mathrm{ext}_\varpi(\varpi\rho_x - K) = \frac{1}{2}\frac{\beta_*}{\rho^{\gamma+1}}\rho_x^2 - U = \frac{1}{2}m(\rho)\rho_x^2 - U. \tag{B3}$$

The Euler–Lagrange equation reduces to (39). Thus, we have Hamiltonian and Lagrangian formulations for both the full R-gas dynamic field equations and their reduction to the space of steady solutions.

APPENDIX C: PARABOLIC EMBEDDING AND LAGRANGE–JACOBI IDENTITY FOR STEADY FLOW

For $\gamma \neq 2$, the quadrature in (42) cannot be done using elliptic functions, but could be done numerically. An alternative approach is to take a linear combination of the equations in (38) to obtain a form of the steady equation for ρ without the velocity dependent term, but with a generally non-integral power of ρ,

$$\beta_*\rho_{xx} = (\gamma+1)K\rho^\gamma - 2F^{\rm u}\rho + F^{\rm p}. \tag{C1}$$

If we introduce a pseudo-time τ, then steady solutions can be obtained via a parabolic embedding in a nonlinear heat equation with a source,

$$\rho_\tau - \beta_*\rho_{xx} = -(\gamma+1)K\rho^\gamma + 2F^{\rm u}\rho - F^{\rm p}. \tag{C2}$$

By prescribing suitable BCs and starting with an arbitrary initial condition, the solution of this PDE should relax to the stable solutions of (C1).

Equation (C1) may also be used to derive additional virial/Lagrange–Jacobi-type identities by multiplying it by ρ and using (41) and repeating the process. The first two such identities are

$$\frac{\beta_*}{2}(\rho^2)_{xx} = (\gamma+3)K\rho^{\gamma+1} - 4F^{\rm u}\rho^2 + 3F^{\rm p}\rho - (F^{\rm m})^2$$

and

$$\frac{\beta_*}{3}(\rho^3)_{xx} = (\gamma+5)K\rho^{\gamma+2} - 6F^{\mathrm{u}}\rho^3 + 5F^{\mathrm{p}}\rho^2 - 2(F^{\mathrm{m}})^2\rho. \tag{C3}$$

Integrating (C1) and (C3) with periodic BCs, we get a hierarchy of integral invariants for steady solutions

$$\begin{aligned}&\int_{-L}^{L}\left[(\gamma+1)K\rho^{\gamma} - 2F^{\mathrm{u}}\rho + F^{\mathrm{p}}\right]dx\\ &= \int_{-L}^{L}\left[(\gamma+3)K\rho^{\gamma+1} - 4F^{\mathrm{u}}\rho^2 + 3F^{\mathrm{p}}\rho - (F^{\mathrm{m}})^2\right]dx\\ &= \int_{-L}^{L}\left[(\gamma+5)K\rho^{\gamma+2} - 6F^{\mathrm{u}}\rho^3 + 5F^{\mathrm{p}}\rho^2 - 2(F^{\mathrm{m}})^2\rho\right]dx\\ &= 0, \quad \text{etc.}\end{aligned} \tag{C4}$$

These integral identities can provide valuable checks on any numerics used to obtain steady solutions.

APPENDIX D: SEMI-IMPLICIT SPECTRAL SCHEME FOR TIME EVOLUTION

Here, we describe the scheme used to solve the IVP for the 1D $\gamma = 2$ isentropic R-gas dynamic equations (79). To include the effects of the nonlinear terms in (79), we discretize time $\hat{t} = j\Delta$, $j = 0, 1, 2, \ldots$, denote the Fourier modes $\rho_n(j\Delta) = \rho_n^j$, and use a centered difference scheme for the linear part,

$$\begin{aligned}\rho_n^{j+1} &= \rho_n^j - \frac{in\Delta}{2}\left(\bar{u}(\rho_n^j + \rho_n^{j+1}) + u_n^j + u_n^{j+1}\right) - \Delta\delta(\mathscr{F}^{\mathrm{m}})_n^j,\\ u_n^{j+1} &= u_n^j - \frac{in\Delta}{2}\left(\bar{u}(u_n^j + u_n^{j+1}) + (1+\varepsilon^2 n^2)(\rho_n^j + \rho_n^{j+1})\right) - \Delta\delta(\mathscr{F}^{\mathrm{u}})_n^j.\end{aligned} \tag{D1}$$

For simplicity, the nonlinear terms are treated explicitly; treating the linear terms explicitly leads to numerical instabilities. In matrix form, the equations read

$$A\begin{pmatrix}\rho_n^{j+1}\\ u_n^{j+1}\end{pmatrix} = B\begin{pmatrix}\rho_n^{j}\\ u_n^{j}\end{pmatrix} - \Delta\delta\begin{pmatrix}(\mathscr{F}^{\mathrm{m}})_n^j\\ (\mathscr{F}^{\mathrm{u}})_n^j\end{pmatrix},$$

where

$$A = I + \frac{in\Delta}{2}\begin{pmatrix}\bar{u} & 1\\ p_n^2 & \bar{u}\end{pmatrix} \quad \text{and} \quad B = I - \frac{in\Delta}{2}\begin{pmatrix}\bar{u} & 1\\ p_n^2 & \bar{u}\end{pmatrix} \tag{D2}$$

with $p_n^2 = (1+\varepsilon^2 n^2)$. B is related to A via conjugation or by $\Delta \to -\Delta$. Thus, the variables at the $j+1$st time step are

$$\begin{pmatrix}\rho_n^{j+1}\\ u_n^{j+1}\end{pmatrix} = U\begin{pmatrix}\rho_n^{j}\\ u_n^{j}\end{pmatrix} - \Delta\delta A^{-1}\begin{pmatrix}(\mathscr{F}^{\mathrm{u}})_n^j\\ (\mathscr{F}^{\mathrm{u}})_n^j\end{pmatrix},$$

where

$$U = A^{-1}B = \frac{1}{\det A}\left[I + n\Delta\begin{pmatrix}\frac{\Delta}{4}n(\bar{u}^2 - p_n^2) & -i\\ -ip_n^2 & \frac{\Delta}{4}n(\bar{u}^2 - p_n^2)\end{pmatrix}\right],$$

$$(\det A)\,A^{-1} = I + \frac{in\Delta}{2}\begin{pmatrix}\bar{u} & -1\\ -p_n^2 & \bar{u}\end{pmatrix},$$

and

$$\det A = \left(1 + \frac{in\bar{u}\Delta}{2}\right)^2 + \frac{n^2\Delta^2 p_n^2}{4}. \tag{D3}$$

U is unitary with respect to the inner product $\langle(\rho,u),(\tilde{\rho},\tilde{u})\rangle = p_n^2\rho^*\tilde{\rho} + u^*\tilde{u}$, which ensures that the linear evolution conserves H_1 of (35). An advantage of this scheme is that conservation of $\int\rho dx$ and $\int u dx$ is automatically satisfied to round-off accuracy. We also find that Q_r and Q_i (96) are quite accurately conserved in our numerical evolution for the ICs in Sec. VI B. Moreover, since $\mathscr{F}^{\mathrm{m}}$ (75) and $\mathscr{F}^{\mathrm{u}}$ (77) are divergences, their Fourier coefficients can be calculated by integration by parts without any differentiation.

REFERENCES

[1] G. B. Whitham, *Linear and Nonlinear Waves* (Wiley, New York, 1974).
[2] M. J. Ablowitz, *Nonlinear Dispersive Waves Asymptotic Analysis and Solitons* (Cambridge University Press, Cambridge, 2011).
[3] G. Biondini, G. A. El, M. A. Hoefer, and P. D. Miller, "Dispersive hydrodynamics: Preface," Physica D **333**, 1 (2016).
[4] G. A. El and M. A. Hoefer, "Dispersive shock waves and modulation theory," Physica D **333**, 11 (2016).
[5] A. Ali and H. Kalisch, "Energy balance for undular bores," C. R. Mec. **338**, 67 (2010).
[6] A. Thyagaraja, "Conservative regularization of ideal hydrodynamics and magnetohydrodynamics," Phys. Plasmas **17**, 032503 (2010).
[7] G. S. Krishnaswami, S. Sachdev, and A. Thyagaraja, "Local conservative regularizations of compressible MHD and neutral flows," Phys. Plasmas **23**, 022308 (2016); arXiv:1510.01606.
[8] G. S. Krishnaswami, S. Sachdev, and A. Thyagaraja, "Conservative regularization of compressible dissipationless two-fluid plasmas," Phys. Plasmas **25**, 022306 (2018); arXiv:1711.05236.
[9] B. B. Kadomtsev and V. I. Petviashvili, "On the stability of solitary waves in weakly dispersive media," Sov. Phys. Dokl. **15**, 539 (1970).
[10] C. S. Gardner, "Korteweg-de Vries equation and generalizations. IV. The Korteweg-de Vries equation as a Hamiltonian system," J. Math. Phys. **12**, 1548 (1971).
[11] A. Ali and H. Kalisch, "On the formulation of mass, momentum and energy conservation in the KdV equation," Acta Appl. Math. **133**(1), 113 (2014).
[12] A. Karczewska, P. Rozmej, and E. Infeld, "Energy invariant for shallow-water waves and the Korteweg-de Vries equation: Doubts about the invariance of energy," Phys. Rev. E **92**, 053202 (2015).
[13] J. D. van der Waals, "The thermodynamic theory of capillarity under the hypothesis of a continuous variation of density," J. Stat. Phys. **20**, 200 (1979), original work published 1893, translated by J. S. Rowlinson.
[14] D. J. Korteweg, "Sur la forme que prennent les équations du mouvements des fluids si l'on tient compte des forces capillaires causées par des variations de densité," Arch. Néerl. Sci. Exactes Nat. Ser. II **6**, 1 (1901).
[15] J. E. Dunn and J. Serrin, "On the thermomechanics of interstitial working," Arch. Ration. Mech. Anal. **88**, 95 (1985).
[16] A. N. Gorban and I. V. Karlin, "Beyond Navier-Stokes equations: Capillarity of ideal gas," Contemp. Phys. **58**(1), 70 (2017).
[17] T. B. Benjamin, "Upstream influence," J. Fluid Mech. **40**, 49 (1970).
[18] D. Bohm, "A suggested interpretation of the quantum theory in terms of "hidden variables" I," Phys. Rev. **85**, 166 (1952).
[19] E. P. Gross, "Structure of quantized vortex in boson systems," Nuovo Cimento **20**(3), 454 (1961).
[20] E. Madelung, "Quantentheorie in hydrodynamischer form," Z. Phys. **40**, 322 (1927).
[21] B. Bertini, M. Collura, J. De Nardis, and M. Fagotti, "Transport in out-of-equilibrium XXZ chains: Exact profiles of charges and currents," Phys. Rev. Lett. **117**, 207201 (2016).
[22] O. A. Castro-Alvaredo, B. Doyon, and T. Yoshimura, "Emergent hydrodynamics in integrable quantum systems out of equilibrium," Phys. Rev. X **6**, 041065 (2016).
[23] M. Schemmer, I. Bouchoule, B. Doyon, and J. Dubail, "Generalized hydrodynamics on an atom chip," Phys. Rev. Lett. **122**, 090601 (2019).

[24]L. D. Faddeev and L. A. Takhtajan, *Hamiltonian Methods in the Theory of Solitons*, Classics in Mathematics (Springer, Berlin, 2007).
[25]P. J. Morrison and J. M. Greene, "Noncanonical Hamiltonian density formulation of hydrodynamics and ideal magnetohydrodynamics," Phys. Rev. Lett. **45**, 790 (1980); Erratum **48**, 569 (1982).
[26]A. Clebsch, "Ueber die integration der hydrodynamischen gleichungen," J. Reine Angew. Math. **56**, 1 (1859).
[27]V. E. Zakharov and E. A. Kuznetsov, "Hamiltonian formalism for nonlinear waves," Phys.-Usp. **40**(11), 1087 (1997).
[28]H. Bateman, "Notes on a differential equation which occurs in the two-dimensional motion of a compressible fluid and the associated variational problems," Proc. R. Soc. A **125**, 598 (1929).
[29]A. Thellung, "On the hydrodynamics of non-viscous fluids and the theory of helium II. Part II," Physica **19**, 217 (1953).
[30]E. C. G. Sudarshan and N. Mukunda, *Classical Dynamics: A Modern Perspective* (Hindustan Book Agency, New Delhi, 2016).
[31]V. Ermakov, "Second order differential equations. *Conditions of complete integrability*," Univ. Izv. Kiev Ser. III **9**, 1 (1880) (English translation). A. O. Harin, "Redactor: Leach PGL," Appl. Anal. Discrete Math. **2**, 123 (2008).
[32]E. Pinney, "The nonlinear differential equation $y''(x) + p(x)y + cy^{-3} = 0$," Proc. Am. Math. Soc. **1**, 681 (1950).
[33]M. Abramowitz and I. A. Stegun (Dover Publications, New York, 1965).
[34]N. J. Zabusky and M. D. Kruskal, "Interaction of "solitons" in a collisionless plasma and the recurrence of initial states," Phys. Rev. Lett. **15**, 240 (1965).
[35]A. Thyagaraja, "Recurrent motions in certain continuum dynamical systems," Phys. Fluids **22**, 2093 (1979).
[36]A. Thyagaraja, in *Recurrence Phenomena and the Number of Effective Degrees of Freedom in Nonlinear Wave Motion*, edited by L. Debnath (Cambridge University Press, 1983), Chap. 17, pp. 308–325.
[37]A. Sen, D. Ahalpara, A. Thyagaraja, and G. S. Krishnaswami, "A KdV-like advection-dispersion equation with some remarkable properties," Commun. Nonlinear Sci. Numer. Simul. **17**, 4115 (2012).
[38]L. P. Pitaevskii, "Vortex lines in an imperfect bose gas," Sov. Phys. JETP **13**(2), 451 (1961).
[39]L. A. Turski, "Hydrodynamical description of the continuous Heisenberg chain," Can. J. Phys. **59**(4), 511 (1981).
[40]M. Lakshmanan, T. W. Ruijgrok, and C. J. Thomson, "On the dynamics of a continuum spin system," Physica A **84**, 577 (1976).
[41]S. Novikov, S. V. Manakov, L. P. Pitaevskii, and V. E. Zakharov, *Theory of Solitons—The Inverse Scattering Method* (Consultants Bureau-Plenum Publishing Corporation, New York, 1984).
[42]P. D. Miller, "On the generation of dispersive shock waves," Physica D **333**, 66 (2016).
[43]T. Tao, *Nonlinear Dispersive Equations: Local and Global Analysis*, CBMS Regional Conference Series in Mathematics (American Mathematical Society, Rhode Island, 2006), Vol. 106.
[44]T. Tao, "Global behaviour of nonlinear dispersive and wave equations," Current Dev. Math. **2006**, 255.
[45]S. Hatland and H. Kalisch, "Wave breaking in undular bores generated by a moving weir," Phys. Fluids **31**, 033601 (2019).
[46]D. L. Wilkinson and M. L. Banner, "Undular bores," in 6th Australian Hydraulics and Fluid Mechanics Conference, Adelaide, Australia, 1977.
[47]S. G. Rajeev, *Fluid Mechanics, A Geometrical Point of View* (Oxford University Press, Oxford, 2018).
[48]A. Ali and H. Kalisch, "Reconstruction of the pressure in long-wave models with constant vorticity," Eur. J. Mech.: B/Fluids **37**, 187 (2013).
[49]F. Huang, Y. Wang, Y. Wang, and T. Yang, "Justification of limit for the Boltzmann equation related to Korteweg theory," Q. Appl. Math. **74**, 719 (2016).